Biogeosciences, 8, 1987–2007, 2011
www.biogeosciences.net/8/1987/2011/
doi:10.5194/bg-8-1987-2011

Biogeosciences

Interannual variability of air-sea CO_2 fluxes and carbon system in the East Siberian Sea

I. I. Pipko[1], **I. P. Semiletov**[1,2], **S. P. Pugach**[1], **I. Wåhlström**[3], **and L. G. Anderson**[3]

[1]Pacific Oceanological Institute FEB RAS, Vladivostok, Russian Federation, Russia
[2]International Arctic Research Center/University of Alaska, Fairbanks, USA
[3]Department of Chemistry, University of Gothenburg, Sweden

Received: 19 January 2011 – Published in Biogeosciences Discuss.: 10 February 2011
Revised: 14 July 2011 – Accepted: 15 July 2011 – Published: 22 July 2011

Abstract. Over the past couple of decades it has become apparent that air-land-sea interactions in the Arctic have a substantial impact on the composition of the overlying atmosphere (ACIA, 2004). The Arctic Ocean is small (only ~4 % of the total World Ocean), but it is surrounded by offshore and onshore permafrost which is thawing at increasing rates under warming conditions, releasing carbon dioxide (CO_2) into the water and atmosphere. The Arctic Ocean shelf where the most intensive biogeochemical processes have occurred occupies 1/3 of the ocean. The East Siberian Sea (ESS) shelf is the shallowest and widest shelf among the Arctic seas, and the least studied. The objective of this study was to highlight the importance of different factors that impact the carbon system (CS) as well as the CO_2 flux dynamics in the ESS. CS variables were measured in the ESS in September 2003 and, 2004 and in late August–September 2008. It was shown that the western part of the ESS represents a river- and coastal-erosion-dominated heterotrophic ocean margin that is a source for atmospheric CO_2. The eastern part of the ESS is a Pacific-water-dominated autotrophic area, which acts as a sink for atmospheric CO_2.

Our results indicate that the year-to-year dynamics of the partial pressure of CO_2 in the surface water as well as the air-sea flux of CO_2 varies substantially. In one year the ESS shelf was mainly heterotrophic and served as a moderate summertime source of CO_2 (year 2004). In another year gross primary production exceeded community respiration in a relatively large part of the ESS and the ESS shelf was only a weak source of CO_2 into the atmosphere (year 2008). It was shown that many factors impact the CS and CO_2 flux dynamics (such as river runoff, coastal erosion, primary production/respiration, etc.), but they were mainly determined by the interplay and distribution of water masses that are basically influenced by the atmospheric circulation. In this contribution the air-sea CO_2 fluxes were evaluated in the ESS based on measured CS characteristics, and summertime fluxes were estimated. It was shown that the total ESS shelf is a net source of CO_2 for the atmosphere in a range of 0.4×10^{12} to 2.3×10^{12} g C.

1 Introduction

The Arctic has undergone dramatic change during the past decades. Climate change has led to remarkable environmental alterations in the Arctic Ocean and its surrounding permafrost (ACIA, 2004; Macdonald et al., 2010). Climate parameters that have changed include atmospheric sea-level pressure, wind fields, sea-ice drift, ice cover, length of melt season, and variation in precipitation patterns and in land hydrology and marine hydrography. It is likely that these primary changes impact the carbon cycle and the biological systems (Vetrov and Romankevich, 2004; Macdonald et al., 2010). The Arctic Ocean's role in determining the regional CO_2 balance has largely been ignored, because of its small size (only ~4 % of the world ocean area) and because its continuous sea-ice cover is usually considered to impede gaseous exchange with the atmosphere so efficiently that no global climate models include CO_2 exchange through sea ice. But recent findings have demonstrated the importance and complexity of ice-related processes in term of CO_2 exchange (Anderson et al., 2004; Semiletov et al., 2004, 2007; Rysgaard et al., 2007; Nomura et al., 2010; Miller et al., 2011;

Correspondence to: I. I. Pipko
(irina@poi.dvo.ru)

Published by Copernicus Publications on behalf of the European Geosciences Union.

Papakyriakou and Miller, 2011), and the Arctic Ocean has attracted increased attention from researchers of the carbon cycle in the context of rapid climate change (e.g. Bates and Mathis, 2009; McGuire et al., 2009; Anderson et al., 2010, 2011).

The coastal ocean plays a disproportionately important role in the ocean's biogeochemical cycle despite its small areal fraction because it acts as a link between terrestrial, atmospheric, and oceanic carbon reservoirs. Input, production, degradation, and export of organic matter (OM) into and out of the coastal ocean are several times higher than in the open ocean (Wollast, 1998). Consequently, it can be expected that the CO_2 exchange between the atmosphere and coastal environments is more intense than in the open ocean and thus is significant for the global carbon budget despite the relatively small surface area of the coastal oceans (Borges et al., 2006). This is especially the situation in the Arctic Ocean where terrestrial and coastal permafrost is a huge reservoir of bioavailable organic carbon (Stein and Macdonald, 2004) that is already involved in the modern biogeochemical cycle (Guo et al., 2004; Semiletov et al., 2007; van Dongen et al., 2008; Anderson et al., 2009; Vonk et al., 2010). The land-shelf-air interaction in the Arctic has a substantial impact on the composition of the overlying atmosphere; as the permafrost thaws, a significant amount of old terrestrial carbon becomes available for biogeochemical cycling and oxidation to CO_2 (Semiletov, 1999a, b; Semiletov et al., 2007).

The Arctic Ocean has the world's largest continental shelf (about 53 % of its area) where the East Siberian Sea (ESS) is its largest and shallowest shelf sea. The issue of whether continental shelves are a sink or a source of atmospheric CO_2, i.e. whether continental shelves are net autotrophic or net heterotrophic, is far from certain (Cai et al., 2003; Macdonald et al., 2010), even for low and temperate latitudes. Despite the vastness of the Arctic shelves, few CS data are available for the ESS except from our previous studies (Olsson and Anderson, 1997; Semiletov, 1999a, b; Pipko et al., 2005, 2008a, b, 2009; Semiletov and Pipko, 2007; Semiletov et al., 2007; Anderson et al., 2009, 2010).

The harsh polar climate and difficulties of logistical support have limited most studies to opportunistic icebreaker surveys conducted on the Arctic shelves during the summertime sea-ice retreat with a couple of transpolar surveys across the deep basin (Bates and Mathis, 2009; Jutterström and Anderson, 2010). As a result, even summer observations of carbon chemistry in the Arctic Ocean are highly sporadic and the absence of repeat hydrographic surveys has considerably constrained our knowledge of the CO_2 sink and source terms in the Arctic Ocean.

In this study we present CS data from the ESS surface water based on surveys conducted in three years (September of 2003 and 2004 and late August–September 2008). The data set obtained is the result of the first and the most comprehensive multiyear study of the CS and CO_2 flux dynamics on the ice-free ESS shelf which was performed using the same methods. Oceanographic stations were carried out over the whole extent of the open sea, from the coast to the ice edge (except for the investigations in September 2003, when stations were placed far south of the ice edge in the western part of the sea). We aim to quantify the importance of individual factors governing CS and CO_2 flux dynamics in the ESS. The spatial and interannual variability of CS characteristics (together with new photosynthetically active radiation (PAR), colored dissolved OM (CDOM), and suspended particulate matter (SPM) data) and metabolic status in the ESS are discussed in relation to variable meteorological regimes, river discharge, and intensity of coastal erosion. Based on the air-sea CO_2 difference and measured wind speed, we compute the air-sea CO_2 flux over the ESS and evaluate its interannual variability. To date, this is the first estimate of the overall CO_2 budget based on multi-year direct summertime measurements of CS parameters.

2 Study area

The ESS is the shallowest marginal sea of the Arctic Ocean. Its average depth is about 54 m, its area is about 913×10^3 km^2, and its volume is about 49×10^3 km^3 (Atlas of the Oceans, 1980). It is, or at least has been, the most inaccessible among all Siberian arctic seas, due to comparatively heavy ice conditions, which often prevented navigation in this region even throughout the summer season. Generally by the end of summer the open sea area is at its maximum and the drifting ice covers about 60–70 % of the area, forming the so-called "Ayon ice massif" in the central ESS (Kulakov et al., 2003). The hydrographical and hydrochemical conditions in the ESS are dominated by Siberian river discharge, ice-related processes (ice formation and melting as well as brine rejection in coastal polynyas), vertical mixing, and exchange with the deep central Arctic Ocean basin and adjacent seas. The ESS can be characterized as an "interior shelf", which is highly influenced by exchanges with other shelves (Carmack et al., 2006).

The Arctic Ocean receives the most river discharge, by far, of the world's oceans (Carmack et al., 2006), but the direct river discharge into the ESS by the Kolyma and Indigirka rivers is small and annually averages only 0.3 % of its volume. A significant part of the ESS freshwater budget is added by Lena River water, which penetrates from the Laptev Sea into the ESS through the Dm. Laptev Strait and straits of the Novosibirsky Islands. Due to the extreme climate the Lena, Indigirka, and Kolyma rivers are characterized by extensive summer floods and a low winter discharge (Fig. 1). About 75–95 % of the discharge occurs during the warm season (http://rims.unh.edu). Note that long-term summer melt water influx into the ESS is about 529 km^3 (Dmitrenko et al., 2008), which is significantly higher than direct river influx into the ESS and is comparable to the annual discharge of the Lena River (535 km^3, http://rims.unh.edu). However,

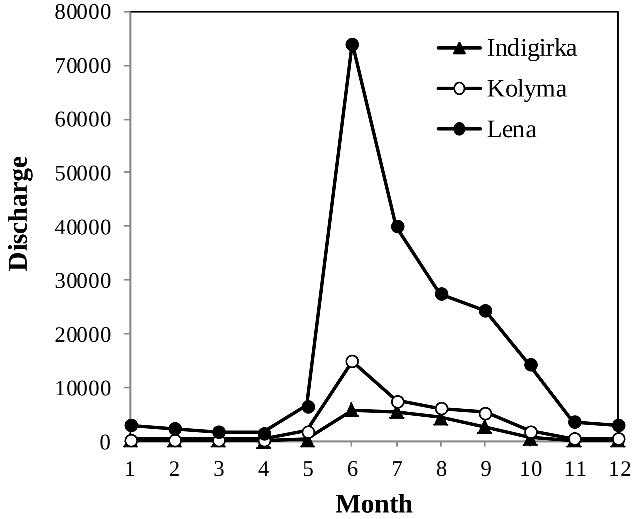

Fig. 1. Monthly average river discharge ($m^3\,s^{-1}$) of the three rivers that dominate the runoff input to the East Siberian Sea.

its annual variability is substantially larger than that of the runoff.

The shallow ESS shelf has the largest gradients in all oceanographic parameters observed for the entire Arctic Ocean (Semiletov et al., 2005). The highest rates of coastal erosion with attendant consequences for offshore flux of eroded material occurs here (Dudarev et al., 2003; Stein and Macdonald, 2004; Grigoriev et al., 2006).

For a major portion of the year, ice cover prevents light from penetrating deep into the water column and thus limits primary production (PP). The ESS has a shorter season of PP mainly because of harsh ice conditions (the ice-free period is about 60–75 days) (Vinogradov et al., 2000). Coastal erosion and river discharges provide a major source of suspended matter and nutrients. The Lena River annually adds substantial amounts of nutrients to the Laptev Sea (2.2×10^6, 2.2×10^4, 2.1×10^4, and 4.2×10^3 tons of SiO_2, NO_3^-, NH_4^+, and PO_4^{3-}, respectively), resulting in a negligible limitation of PP by nutrients (Gordeev et al., 1996). However, over the western ESS shelf substantial input of terrestrial matter leads to low light conditions in the water column even during summer season (Semiletov et al., 2007; Pipko et al., 2008b).

At the present time no consensus exists on the productivity of EES water due to the limited amount of data. The ESS is considered as an oligotrophic or a low-productivity ecosystem (Sorokin and Sorokin, 1996; Vinogradov et al., 2000). Anderson et al. (2011) computed the ESS annual PP based on consumption of dissolved inorganic carbon and evaluated its magnitude to be $\sim 4(\pm 10) \times 10^{12}$ g C if integrated over half of the ESS area. Other estimations of the ESS annual PP are between 10 and 15×10^{12} g C (Vinogradov et al., 2000; Vetrov and Romankevich, 2004; Berger and Primakov, 2007). The maximal value of total PP in the ESS was estimated to be 45×10^{12} g C (Sakshaug, 2004), but the latter number is highly uncertain because it was calculated by extrapolating data from the highly-productive surrounding shelf seas.

The ESS shoreline is one of the shortest among the arctic seas (Grigoriev and Rachold, 2003; Rachold, 2004) but the ESS receives the largest organic carbon input, originated from eroded coastal permafrost deposits (2.2×10^{12} g C yr^{-1}) (Grigoriev et al., 2006). The ESS is the only arctic shelf sea into which coastal organic carbon input slightly exceeds riverine input (1.86×10^{12} g C yr^{-1}) (Stein and Macdonald, 2004). Thus, the terrestrial input of OM is similar in magnitude to PP and likely has increased lately due to permafrost thawing and the retreat of seasonal sea-ice coverage, which increases wave-based shoreline erosion (Serreze et al., 2000).

Models and geophysical data indicate that large areas of the Arctic shelves (including the ESS) are thought to be almost entirely underlain by subsea permafrost from the coastline down to a water depth of about 100 m, as a result of their exposure to the atmosphere during the Last Glacial Maximum (Romanovskii et al., 2005; Shakhova et al., 2010a). It has been found that the ESS sub-sea bottom permafrost is eroding at quite a high rate, ranging from 1 to 15 cm yr^{-1} (Grigoriev, 2006; Razumov, 2010). As a whole, the dynamics of sub-sea permafrost is still poorly known, due mainly to the lack of direct observations (Rachold et al., 2007; Gavrilov, 2008).

The geographic location of the ESS is unique; it is situated on the eastern Siberian Arctic shelf within the zero vorticity contour separating two dominant large-scale centers of atmospheric circulation over the Arctic Ocean (Nikiforov and Shpaikher, 1980; Proshutinsky and Johnson, 1997; Johnson and Polyakov, 2001). During anticyclonic circulation phases the high sea level pressure (SLP) centered in the western Arctic (the Siberian High) is well developed and the Icelandic Low is suppressed. During cyclonic phases the SLP in the western Arctic is weaker and the Icelandic Low is stronger, extending farther into the Barents and Kara seas (Johnson and Polyakov, 2001). Therefore, the oceanographic state of the ESS is sensitive to the dominant atmospheric circulation mode. The response of the ESS to changes in atmospheric pressure is manifested by the redistribution of surface waters (Nikiforov and Shpaiher, 1980). Under the anticyclonic regime along-shore easterly winds dominate the ESS, resulting in an influx of more saline waters from the Chukchi Sea into the ESS; an absence of the Siberian Coastal Current has been detected (Weingartner et al., 1999). Under the cyclonic regime dominant along-shore westerly winds over the entire Laptev Sea and the western ESS introduce an influx of Lena River runoff into the ESS (Dmitrenko et al., 2005); during this period freshened Siberian Coastal Current water was observed in the Chukchi Sea.

Wind-caused waves are comparatively weakly developed in the ESS due to the ice cover extent and the shallow water.

Table 1. Dates of cruises in the ESS.

Cruise	Date
Ivan Kireev 2003	12–20 September
Ivan Kireev 2004	1–14 September
Yakob Smirnitskiy 2008	29 August–5 September
	9–16 September

With ice retreating northward during the period from July to September, the frequency of strong waves increases and is at a maximum in September. At this time the wave heights can be up to 5 m (our observations); waves of this size have the potential to mix the water column from top to bottom in the shallow areas (depth <30 m), causing resuspension of fine bottom material. Along with the increasing frequency of Arctic cyclones and strong storm events (Serreze et al., 2000; ACIA, 2004) and less ice coverage, this mixing might be a factor contributing to additional warming of surface sediments and causing further thawing of permafrost, leading to bottom erosion.

3 Materials and methods

Hydrographic observations and sampling were carried out in the ESS during September 2003 and 2004 and August–September 2008 (Table 1, Fig. 2). Seawater samples were collected in Niskin bottles mounted on a conductivity-temperature-depth (CTD) rosette and then transferred into smaller bottles for chemical analysis. pH was determined potentiometrically and reported on the total hydrogen ion concentration scale (DOE, 1994). The precision of the pH measurements was about ± 0.004 pH units. Direct comparison between potentiometric and spectrophotometric pH measurements (both in "total" scale) was carried out in September 2008. Potentiometric analyses were performed at temperature 20 °C and the spectrophotometric data were recalculated to 20 °C. Results of this comparison demonstrate a good coincidence between two methods ($r = 1.00$, $n = 45$). Furthermore in 2008 the CO_2-system was over determined, dissolved inorganic carbon (C_T), total alkalinity (A_T) and pH, and computations using the different constituents showed good pH accuracy as C_T and A_T were calibrated versus certified reference materials (CRMs), supplied by Andrew Dickson, Scripps Institution of Oceanography.

In September 2003 and 2004 samples for total alkalinity (A_T) were determined as proposed in DOE (1994). The A_T samples were poisoned with a mercuric chloride solution at the time of sampling. Samples were kept in the dark and were analyzed in the lab within one month using an indicator titration method in which 25 ml of seawater was titrated with 0.02 M HCl in an open cell according to Bruevich (1944). In 2000 the Carbon Dioxide in the Ocean working group of the North Pacific Marine Science Organization (PICES) performed an intercalibration of A_T in seawater using CRMs. The results of the intercalibration showed that the alkalinity values obtained by the Bruevich method are in agreement with the standard within $\pm 1\ \mu mol\ kg^{-1}$ when state-of-the-art analytical practice is applied (Pavlova et al., 2008).

In August–September 2008 A_T was determined after pH from the same sample on board the "Yakob Smirnitskiy", using an open-cell potentiometric titration method. HCl of 0.05 M concentration was used and the endpoint was determination by a Gran function (Haraldsson et al., 1997). The concentrations thus obtained were calibrated against CRMs. The precision of both titration methods was similar at about 0.1 %.

During the 2003–2004 cruises a Seabird SBE19plus Profiler (www.seabird.com) was used for measurements of conductivity, temperature, PAR (by LI-193SA Spherical Quantum Sensor), turbidity (by OBS-3 Sensor), and fluorescence (a WetStar fluorimeter was used to assess the in situ CDOM concentration; this instrument has a single excitation ($E_x = 370$ nm)/emission ($E_m = 460$ nm) wavelength pair); these measurements characterized the distribution of CDOM at 0.20 m vertical intervals at the oceanographic stations. Dissolved oxygen (O_2) concentrations were obtained using a Winkler titration system, giving a precision of $\sim 3\ \mu mol\ kg^{-1}$ for 2003–2004 data and $\sim 1\ \mu mol\ kg^{-1}$ for 2008 data. These values were then converted to a percent saturation, following Weiss (1970).

The seawater partial pressure of CO_2 (pCO_2) was computed from pH-A_T using CO2SYS (Lewis and Wallace, 1998). The carbonic acid dissociation constants (K_1 and K_2) of Mehrbach et al. (1973) as refit by Dickson and Millero (1987) were used. The uncertainty in computed pCO_2 was about 10 µatm.

In the 2003 and 2004 cruises atmospheric CO_2 concentration was measured using the non-dispersive infrared LI-820 CO_2 analyzer with accuracy better than 3 % (www.licor.com), while in the 2008 cruise the high-precision open-path LiCor-7500 was used.

The equation published by Wanninkhof and McGillis (1999) was used to calculate the CO_2 flux (F_{CO_2}):

$$F_{CO_2} = K_0 \cdot k \cdot (pCO_2^{sw} - pCO_2^{air}),$$

$$k = 0.0283 \cdot u^3 (660/Sc)^{0.5},$$

where K_0 is the solubility of CO_2 at the in situ temperature (mol m^{-3} atm^{-1}), k is the gas transfer velocity (cm h^{-1}), u is the 10 m wind speed (m s^{-1}), and Sc is the Schmidt number for CO_2 defined by Wanninkhof (1992). The wind speeds used in the calculation of transfer velocity were daily averaged values measured on board during each cruise.

Air-sea flux rates were calculated at each hydrocast station. For calculating the integrated CO_2 flux of the ESS the station data were interpolated onto a uniform grid (Kriging algorithms) using the grid-based graphics program Surfer

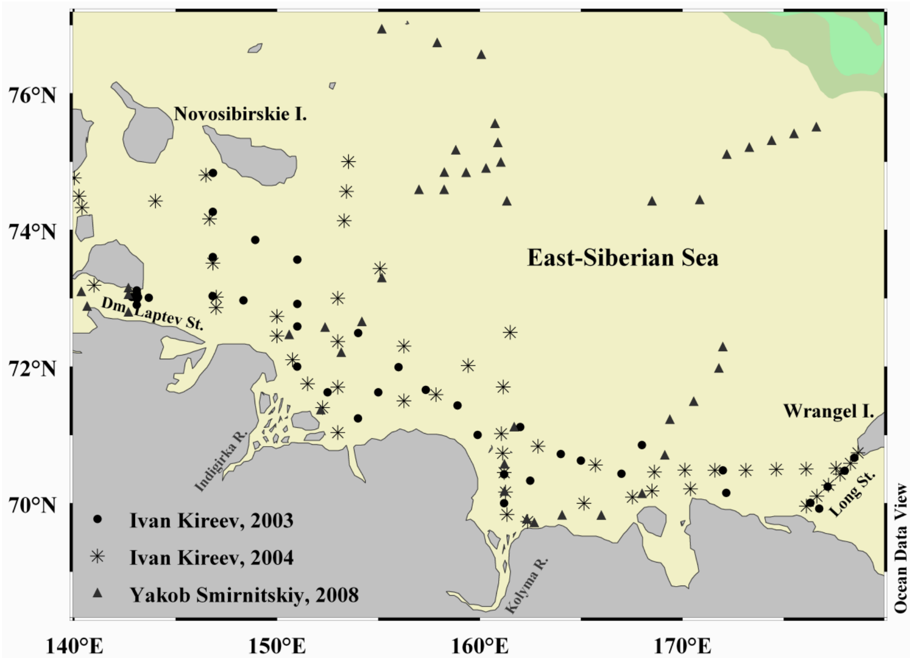

Fig. 2. Map of the stations in the East Siberian Sea during the 2003, 2004, and 2008 surveys.

8.0, and then a modified grid was created using the digitized positions of ice-edge and sea borders (www.aari.ru). Finally, the mean value of the daily CO_2 flux for ice-free sea was evaluated. Note that in 2003 hydrographic station positions were far south of the ice edge, so interpolated data from 2003 were extrapolated to the entire open ESS.

Errors in the integrated CO_2 flux estimations arise from a combination of interpolation and extrapolation errors, from uncertainties in flux parameterizations, and also from errors in the computed $p\mathrm{CO}_2$. Sea ice has to be considered when the total flux of CO_2 is computed because a large fraction of the region is covered by ice. Therefore, additional uncertainties in CO_2 flux computation are caused by the ice edge position.

4 Results

The marine carbon cycle is largely determined by forcing factors such as wind, sea ice, and runoff and hence these conditions are described first.

4.1 Meteorological situation

The National Centers for Environmental Prediction (NCEP) SLP data were employed to describe the atmospheric circulation over the Arctic Ocean (www.esrl.noaa.gov). The SLP fields, averaged over the summer season (July–September) for each year, are shown in Fig. 3 and have substantial interannual variability. During the 2003 summer season cyclonic atmospheric circulation dominated over the central Arctic Ocean. SLP down to 1005 mbar extended into the Laptev and the East Siberian seas. In 2004 the summer low pressure north of the ESS was weaker while an anticyclone, located above the Canadian Arctic Archipelago, formed. In contrast to the situation in 2003–2004, during the 2008 warm season an anticyclone dominated over the Canada Basin of the central Arctic Ocean and a low pressure center was present over Siberia.

4.2 Ice conditions

Our investigations were carried out in the late August-September period of maximal seasonal sea-ice retreat. During all cruises the ice edge was well north of its 1979–2000 median September position and well off the coast of Siberia. The second-lowest sea-ice extent shown in the satellite record occurred in 2008 (http://nsidc.org/news/press/). Figure 4 illustrates sea-ice extent in the ESS during the period of the three expeditions (ice charts were obtained from www.aari.ru). In September 2008 the ice-free area covered about 95 % of the ESS area, in September 2003 it covered about 70 %, and in September 2004 it covered about 50 % of the ESS.

4.3 Hydrography

As stated earlier by Proshutinsky and Johnson (1997) the circulation in the ESS is driven by dominating winds, which can be deduced from the pressure field shown in Fig. 3. Dmitrenko et al. (2005) also note that at the average shelf depth of about 20–25 m the wind-forced flow is essentially

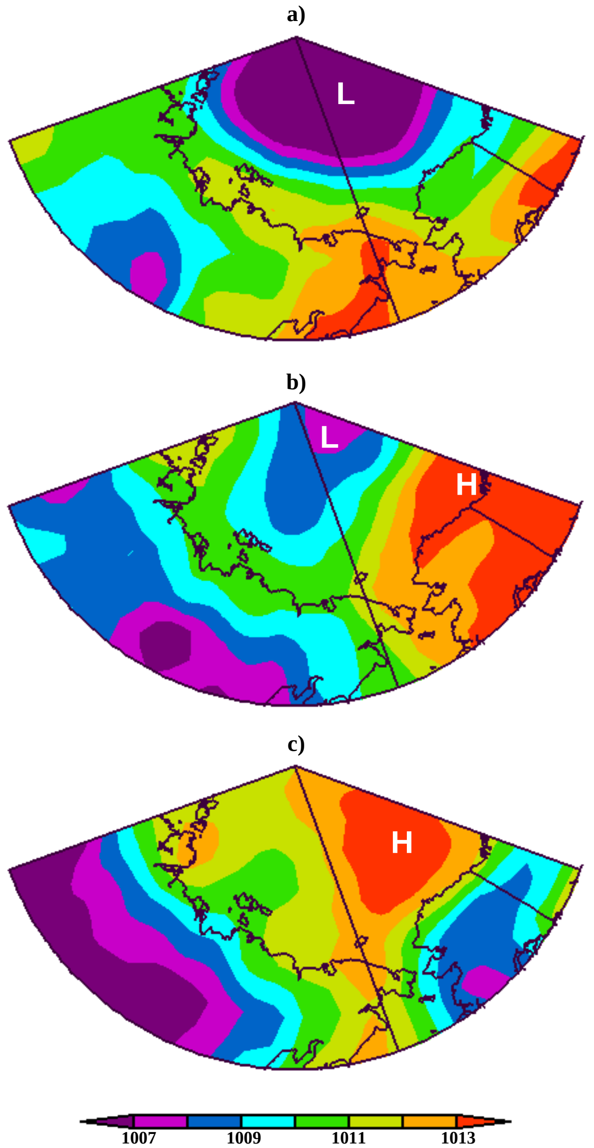

Fig. 3. Sea level pressure fields (mbar), averaged over the summer season (July–September) in 2003 **(a)**, 2004 **(b)**, and 2008 **(c)**, from NCEP data.

controlled by wind stress and bottom friction; the Coriolis force becomes insignificant, and the surface current aligns almost completely with the wind direction. The spatial distribution of sea-surface salinity and temperature obtained in 2003, 2004, and 2008 is shown in Fig. 5. In Fig. 6 sections of density, expressed as sigma ($\sigma = 1000 \times$ (density-1)), are shown for the along-shore transects.

The overall hydrographic conditions in the coastal zone were mainly characterized by the interaction of warm and fresh waters from the Indigirka (152° E) and Kolyma (162° E) rivers with brackish waters from the Laptev Sea and the relatively cold and saline water of Pacific origin from the Chukchi Sea (Fig. 5). The sea-surface salinity showed a general eastward increasing trend. Summer observations of salinity varied between 8.49 (2004) and 30.39 (2008), but the latter was to the northeast at the shelf break. Surface temperature values ranged from −0.99 °C (2008) to 6.59 °C (2008), increasing, in general, from Long Strait to Dm. Laptev Strait, and also near the river mouths. The freshwater signal from the Kolyma and Indigirka rivers was detected by minimum salinity (∼8.49, 2004) and high temperature (up to 6.17 °C, 2004). The 25 isohaline has been reported to be a "conventional" boundary of river water propagation (Antonov, 1957). The maximum eastward spreading of river water was detected in September 2004 when the freshwater signal was found in the vicinity of Long Strait. In contrast, in the summer of 2008 freshened waters were shifted in the opposite direction, to the western part of the ESS. The lack of a low-salinity band along the coast in 2008 showed that the Siberian Coastal Current was not established this year, which was a result of changes in the atmospheric circulation pattern as shown in Fig. 3. The spreading of freshened ESS shelf waters is also seen in the strong horizontal and vertical density gradients in the eastern part of the ESS in September 2003 and 2004 (Fig. 6). In contrast, sharp vertical and horizontal gradients were observed in the western ESS in late August–September 2008. In September 2003 and 2004 the water column in the western ESS near Dm. Laptev Strait was found to be almost homogenous, whereas in 2008 density increased with depth.

4.4 Distributions of surface water carbon system parameters

The distributions of the CS parameters ($pH_{in\,situ}$, A_T, total alkalinity normalized to $S = 35$ (nA_T), and pCO_2) in the ESS surface waters are shown in Figs. 7 and 8. The concentration of surface A_T values ranged widely (0.867–2.221 mmol kg^{-1}) with similar spatial gradients as surface salinity, i.e. the lowest values at stations where large amounts of river water diluted A_T and salinity. There were also large variations in surface seawater $pH_{in\,situ}$ distribution on the ESS shelf (7.48–8.34 units). Maximum values of A_T and $pH_{in\,situ}$ were observed in the eastern part of the ESS, and values measured in September 2008 were the highest values obtained during all three surveys (Fig. 7). The lowest surface values of A_T and pH were found over the ESS shelf in the summer of 2004. Variations in nA_T were greatest in the summer of 2008 when these values ranged from 2.336 up to 3.641 mmol kg^{-1}. The observed features in the CS parameters largely reflect the hydrological characteristics as described above.

The pCO_2 data show strong and varying deviation from atmospheric CO_2 in the summer, both between the years and in space. In September 2003 the pCO_2 values in the surface layer varied from 252 to 521 µatm, in 2004 from 272 to 1033 µatm, and in 2008 from 198 to 905 µatm (Fig. 8). The observations showed a clear and stable tendency in the

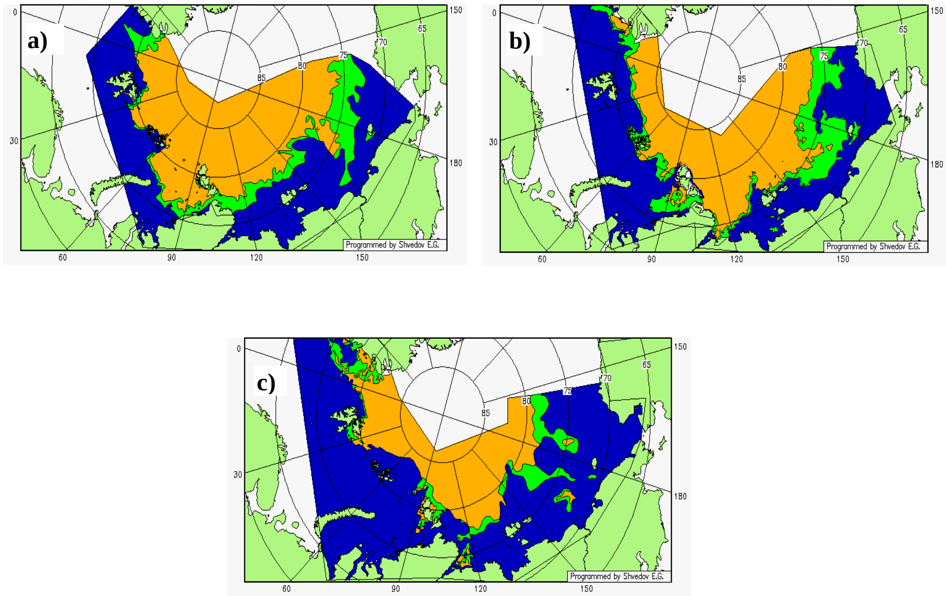

Fig. 4. Sea-ice extent in the Eurasian Arctic Seas during expeditions dated: September 2003 **(a)**, 2004 **(b)**, and 2008 **(c)**, from AARI data. Blue is open water, green is 1/10 to 6/10 ice coverage, and orange is 7/10 to 10/10 ice coverage.

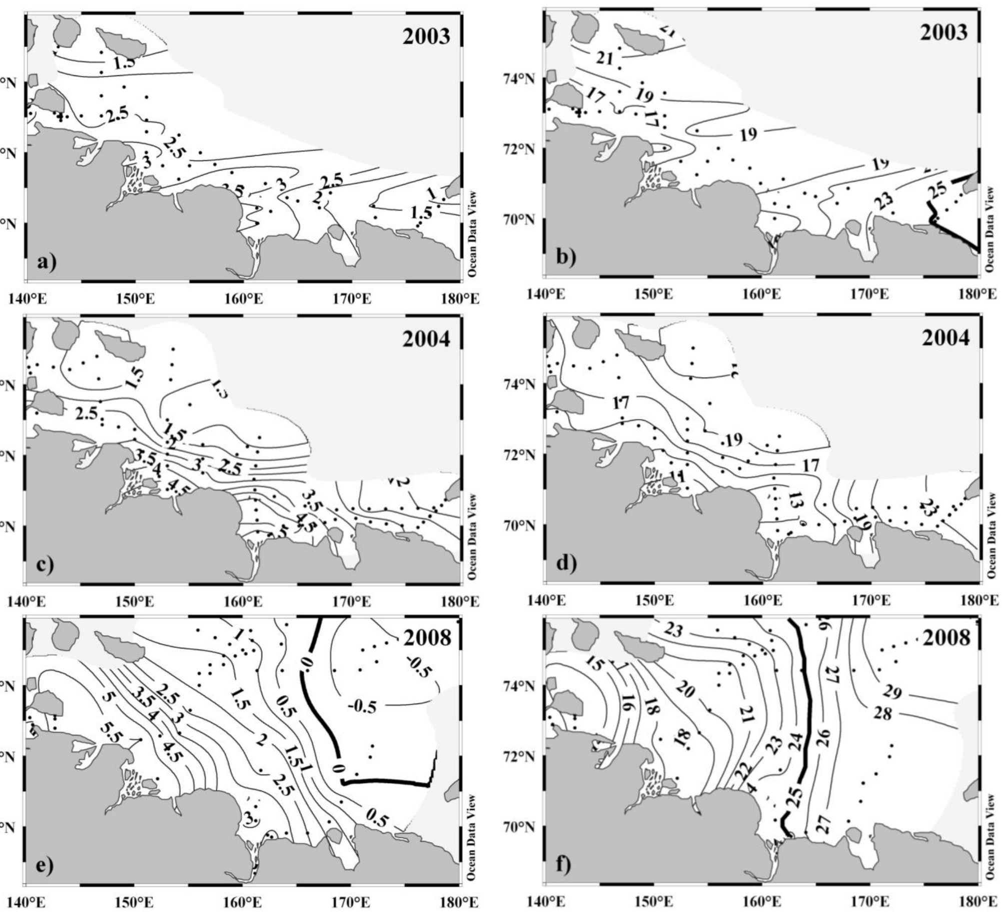

Fig. 5. Spatial distributions of sea surface temperature (°C) **(a, c, e)** and salinity **(b, d, f)** in the ESS during the 2003, 2004, and 2008 surveys.

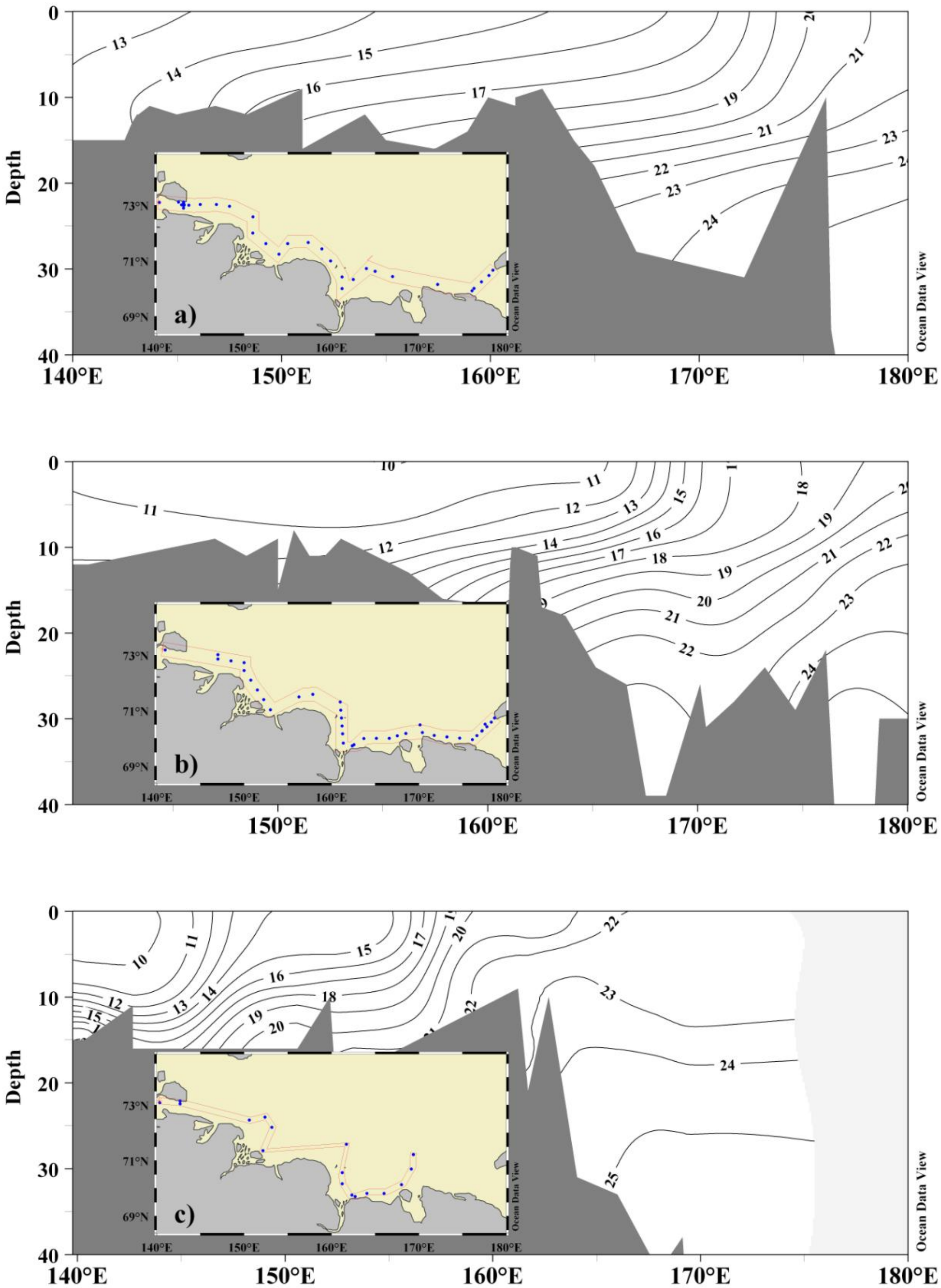

Fig. 6. Profiles of density, expressed as $\sigma = 1000 \times$ (density-1), (kg m^{-3}) on the alongshore transects in September 2003 **(a)**, 2004 **(b)**, and 2008 **(c)**.

spatial distribution of $p\mathrm{CO}_2$ in the surface layer of the ESS; a decrease from the west to the east and considerable fluctuations near estuaries and eroding shorelines. In the western part the surface water was oversaturated with CO_2, and in the east the $p\mathrm{CO}_2$ values were significantly lower than atmospheric values (Fig. 8).

4.5 Air-sea fluxes of CO_2

The distributions of computed air-sea fluxes of CO_2 are illustrated in Fig. 9, and the statistics for positive and negative CO_2 fluxes, calculated from individual flux values at each station, are listed in Table 2. The general characteristics of the CO_2 flux distributions measured during the three cruises

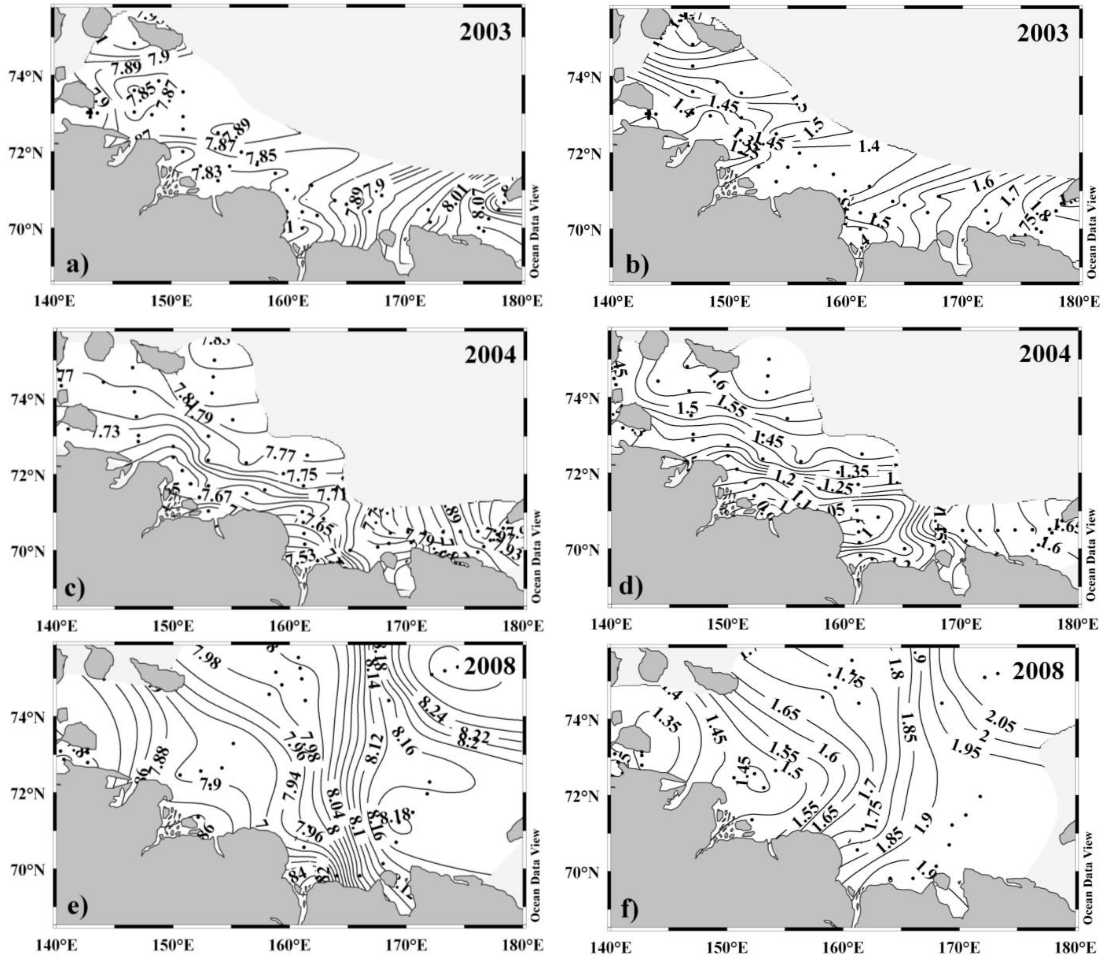

Fig. 7. Spatial distributions of surface water $pH_{in\ situ}$ **(a, c, e)**, and total alkalinity, A_T ($mmol\,kg^{-1}$) **(b, d, f)**, in the ESS during the 2003, 2004, and 2008 surveys.

Table 2. Averaged values of the difference in partial pressures of CO_2 between the surface water and atmosphere (ΔpCO_2) for the regions of under- (invasion, inv) and over- (evasion, ev) saturation relative to the atmosphere, the CO_2 flux for these two regions (F_{CO_2}), and the daily average wind speed (U), for all oceanographic stations visited in the ESS in 2003, 2004, and 2008.

Year	ΔpCO_{2inv}, µatm	ΔpCO_{2ev}, µatm	FCO_{2inv}, $mmol\,m^{-2}\,day^{-1}$	FCO_{2ev}, $mmol\,m^{-2}\,day^{-1}$	U, $m\,s^{-1}$
2003	-44 ± 42, $n = 9$	69 ± 47, $n = 32$	-0.8 ± 0.8, $n = 9$	1.6 ± 1.5, $n = 32$	4.0 ± 0.8, $n = 41$
2004	-35 ± 44, $n = 4$	196 ± 103, $n = 62$	-1.7 ± 2.1, $n = 4$	10.2 ± 8.1, $n = 62$	5.7 ± 1.7, $n = 66$
2008	-95 ± 68, $n = 32$	135 ± 163, $n = 33$	-1.7 ± 1.4, $n = 32$	5.0 ± 5.3, $n = 33$	4.4 ± 1.3, $n = 65$

can be summarized as follows: in the shelf waters the CO_2 fluxes tended to be positive (CO_2 out-gassing) in the western part of the ESS and negative (CO_2 absorption) in the eastern part.

In September 2003 air-sea CO_2 flux rates in the ESS were close to neutral and varied between 4.2 and $-2.0\,mmol\,m^{-2}\,day^{-1}$ (negative values denote an ocean CO_2 sink). The CO_2 flux averaged for the ice-free zone was slightly positive and equal to $0.9 \pm 0.8\,mmol\,m^{-2}\,day^{-1}$.

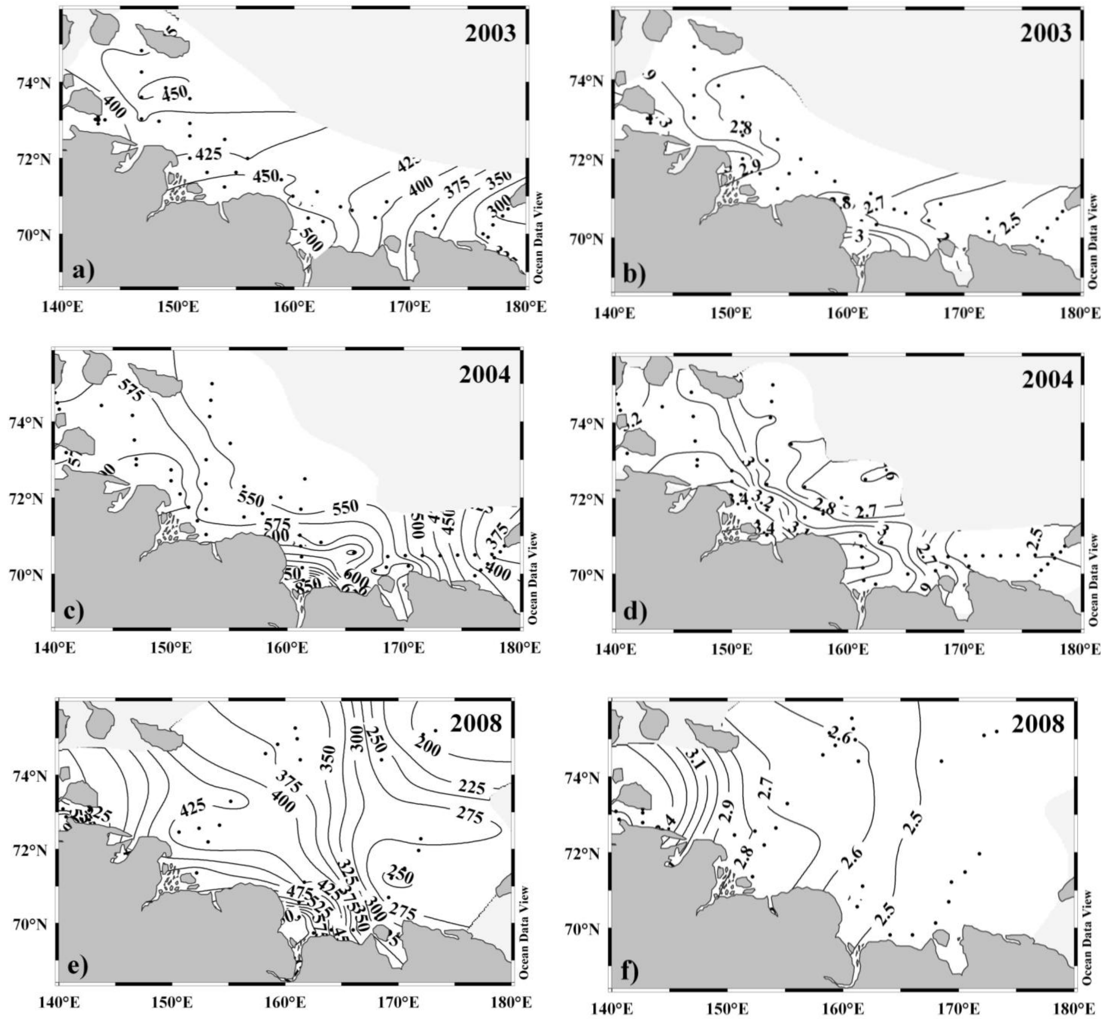

Fig. 8. Spatial distributions of surface water pCO_2 (µatm) **(a, c, e)** and normalized total alkalinity, nA_T (mmol kg^{-1}) **(b, d, f)**, in the ESS during the 2003, 2004, and 2008 surveys.

In September 2004 the ESS shelf had changed from mostly neutral conditions to a modest/strong source of CO_2, and the CO_2 flux into the atmosphere reached 33.2 mmol m^{-2} day^{-1}. The exception was a small region of CO_2 influx in the easternmost part of the ESS in the vicinity of Wrangel Island, where downward CO_2 flux varied from -0.1 to -4.8 mmol m^{-2} day^{-1}. The maximum CO_2 efflux was detected near the Kolyma River mouth (where the highest rates of coastal erosion are also known to occur). The average CO_2 efflux rate from the ESS shelf was a modest 11.5 ± 7.5 mmol m^{-2} day^{-1}.

In late August–September 2008 the CO_2 flux values ranged from -5.0 to 19.4 mmol m^{-2} day^{-1} and the invasion area was the largest measured among the surveys (Fig. 9). The resulting CO_2 flux was close to neutral and equal to 0.8 ± 2.9 mmol m^{-2} day^{-1}.

5 Discussion

The seawater CS is a highly dynamic natural phenomenon which is strongly influenced by many physical and biological processes. As summarized by Bates et al. (2011), the major factors governing seawater CS dynamics are warming/cooling, the balance of evaporation and precipitation, vertical and horizontal mixing, biological uptake/release of CO_2 and alkalinity, and the process of air-sea gas exchange. The CS features of the shallow, biogeochemically-active shelf sea environments reflect strong terrestrial discharge and close interaction between the sedimentary, aquatic, and atmospheric compartments (Thomas et al., 2009). In the polar seas ice-related processes significantly modify the carbon chemistry of seawater. Moreover, another factor influencing the CS dynamics is a strong influx of bioavailable OM as result of coastal (and bottom) permafrost erosion (Semiletov et al, 1999a, b; Guo et al., 2004). This process is especially

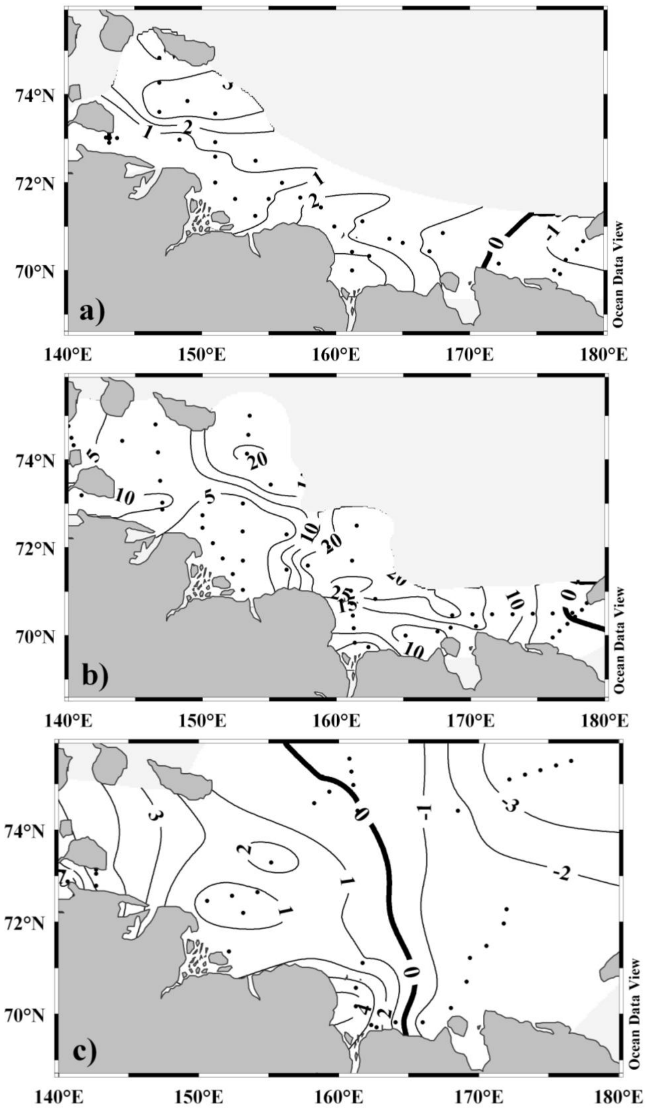

Fig. 9. Spatial distributions of air-sea CO_2 fluxes (mmol m^{-2} day^{-1}) over the ESS shelf during the 2003 **(a)**, 2004 **(b)**, and 2008 **(c)** surveys ("+" – evasion, "−" – invasion).

important for the ESS where the highest rates of coastal erosion in the arctic seas were observed (Grigoriev et al., 2006).

A diversity of processes determines CS dynamics and the exchange of CO_2 on the ESS shelf. We consider some of them below, based on the data set collected over the ESS shelf during the 2003, 2004, and 2008 summer seasons.

5.1 Spatial variability of carbon system parameters

Two hydrological regimes dominate in the ESS, one in the west and one in the east (Semiletov et al., 2005). The distribution of the carbon parameters in the surface water supports this conclusion, but this distribution demonstrates significant year-to-year variability in the location of the invasion/evasion zonal boundaries. In some years the zonal boundary deviates significantly from the long-term (climatic) location of the sediment geochemical boundary and the major reasons determining this variability will be discussed below.

The pCO$_2$ field largely follows the hydrological regimes, with values decreasing from high over-saturation values in the west to under-saturation in the east of the study area (Fig. 8). This decrease in pCO$_2$ is accompanied by a decrease in temperature and an increase in salinity (Fig. 5). The temperature contribution to the west-to-east pCO$_2$ decrease due solely to the temperature reduction (calculated using CO2SYS; Lewis and Wallace, 1998), was 0.041–0.043 °C^{-1}. Hence, about half of the pCO$_2$ change in 2008 can be explained by the temperature variability. For instance the difference between surface water pCO$_2$ in the Dm. Laptev Strait and in the vicinity of Wrangel Island was ∼300 µatm, while the temperature impact ($\Delta T \sim 7$ °C) caused about 147 µatm of this difference. In September 2003 the surface water pCO$_2$ decreased from 491 to 252 µatm over about the same distance while the temperature dependent decrease ($\Delta T \sim 2$ °C) was equal to ∼42 µatm. In September 2004 the temperature effect ($\Delta T \sim 2.5$ °C) was responsible for ∼63 µatm of the pCO$_2$ decrease of ∼387 µatm. The direct impact in pCO$_2$ by salinity is small but there could be other effects from the chemical composition of the freshwater added.

The river runoff has an excess of A_T (e.g. Anderson et al., 2004; Pipko et al., 2008b) as well as of CDOM (Pugach et al., 2009, 2010), where the first is a result of HCO_3^- content and the last a result of dissolved organic carbon (DOC) content. For example, in September 2003 and September 2004 coefficients of linear correlation of A_T-S values and CDOM-S values in surface water along the near-shore transect (position of transects is shown in Fig. 6) were 0.99 and 0.93 (A_T-S) and −0.96 and −0.86 (CDOM-S), respectively. For all data sets the coefficients of linear correlation of A_T-S values in 2003, 2004, and 2008 were 0.99, 0.98, and 0.99, respectively (Fig. 10). Such strong correlation of A_T and CDOM values with salinity, together with the offset at zero salinity, suggests that rivers are strong sources of these components to the ice-free ESS.

However, at least two other freshwater sources, melted sea ice and in-situ precipitation, are also components of the ESS freshwater budget, which complicates the analysis of runoff transport using salinity alone (Cooper et al., 2008). It has been reported that sea ice formation or melting under natural conditions does not fractionate A_T (Anderson and Jones, 1985; Nedashkovsky et al., 2009). Since the A_T in precipitation also is negligible (Cooper et al., 2008) we regard nA_T as a tracer of river water dispersion over the ice-free Arctic shelf. Figures 8 and 11 illustrate that the western part of the ESS was strongly influenced by river input of dissolved inorganic and organic carbon and its annual variability.

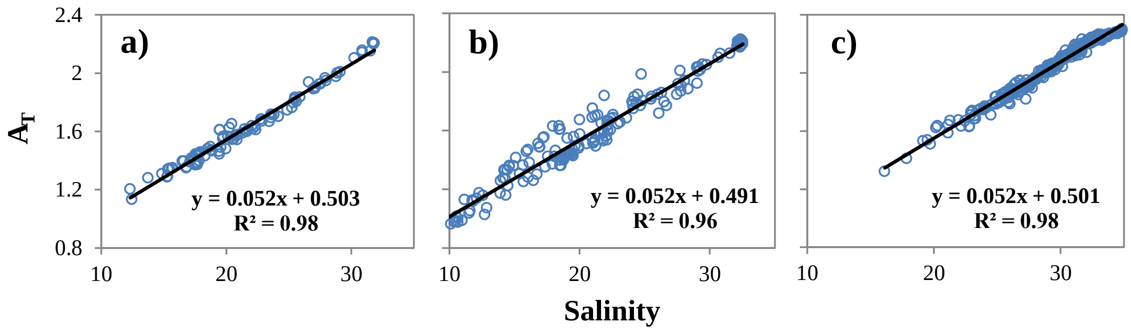

Fig. 10. Relationship between A_T (mmol kg^{-1}) and salinity for samples collected in the ESS in September 2003 **(a)**, September 2004 **(b)**, and August–September 2008 **(c)**.

The impact of runoff on seawater composition is not limited to lowering salinity and increasing nA_T and DOC. Runoff is also characterized by low pH and high $p\mathrm{CO_2}$ (Figs. 7 and 8), the result of decaying terrestrial OM in the drainage basins as well as in the river and its estuaries (Guo et al., 2004; van Dongen et al., 2008; Alling et al., 2010; Sanchez-Garcia et al., 2011; Gustafsson et al., 2011).

The ESS coast line is characterized by the occurrence of ice-rich deposits containing old organic carbon and these deposits are most prevalent in the western part of the sea (Grigoriev et al., 2006). As mentioned above, the erosion rate of these deposits is among the highest in Arctic seas, and remineralization of the eroded OM adds to anomalously high $p\mathrm{CO_2}$. The fact that the OM buried in the permafrost is bioavailable has been confirmed (Semiletov, 1999a, b; Guo et al., 2004; van Dongen et al., 2008; Anderson et al., 2009; Vonk et al., 2010; Sanchez-Garcia et al., 2011). It has been suggested that the major part of the dissolved OM that enters the sea with the river discharge is not biodegradable (Dittmar and Kattner, 2003). However, recent findings suggest that the lability of terrestrial DOC is variable (Alling et al., 2010). Thus, the observed surface water oversaturation relative to the atmospheric CO_2 level in the western part of the ESS is a result of the inflow of warm and turbid, more acidic (in comparison to ocean) river waters with a high CO_2 concentration, as well as to intensive heterotrophic processes taking place because of the large amount of allochthonous bio-available OM added mainly by erosion.

Primary productivity rates in seawater are dependent on the nutrient availability as well as the light (PAR) which penetrates the water column. It is known that attenuation of PAR in the open water column is caused by SPM backscattering as well as adsorption by phytoplankton and CDOM. In regions with considerable river runoff, absorption by CDOM may be ten times greater than that of absorption by phytoplankton (Burenkov et al., 2001). In the western part of the area there was a sharper vertical extinction of PAR compared to in the east and the depth at which the PAR intensity decreased to 1 % of the surface layer values (H_1) deepened from 4–7 m in the western area to 45 m in the eastern area (Fig. 12). This observation coincides well with the decrease in SPM and CDOM concentrations moving from the Dm. Laptev Strait to Long Strait (Fig. 11).

The SPM values (calculated from the turbidity data according to Shakhova and Semiletov, 2008) and CDOM concentrations in the surface waters of the western part of the ESS were one order of magnitude higher than in the eastern part, a result of the high contribution by river runoff and coastal erosion in the west. Intensive wave- and wind-mixing, typical for the shallow south-western ESS, lead to sediment resuspension and might also have added to the observed high SPM concentration (Semiletov et al., 2005; Dudarev et al., 2006). Furthermore, resuspension of heterotrophic bacteria along with SPM can increase the CO_2 concentration in the water column via OM decomposition (Amon and Benner, 1996). In addition to sediments that are resuspended off the seabed, SPM may also originate from a “benthic fluff” layer (Verspecht and Pattiaratchi, 2010) which contains low-density OM that is available for degradation and remineralization. This thin (up to 1 m) near-bottom layer (also called the “nepheloid” layer) enriched in organic carbon has been found in the ESS (Dudarev et al., 2009), and in the Barents Sea (Romankevich et al., 2000). Concentration of organic carbon in this layer is one order of magnitude higher relative to the overlying water (O. V. Dudarev, personal communication, 2010). During a wind event typical of the western part of the ESS during August–September, when seabed shear stress and turbulence are high, the benthic fluff can become homogeneously distributed through the water column and may add a source of SPM (Grigoriev, 2006; Dudarev et al., 2008).

Correlation of H_1 depth against the mean CDOM and SPM values in this H_1 layer along the near-shore transect in 2004 were -0.92 and -0.73, respectively ($n = 16$). Moreover, the rate of the PAR extinction in the H_1 layer showed a close relationship with those parameters (Fig. 13). At stations with similar turbidity but with higher CDOM, the decrease in PAR with depth was greater, which illustrates the

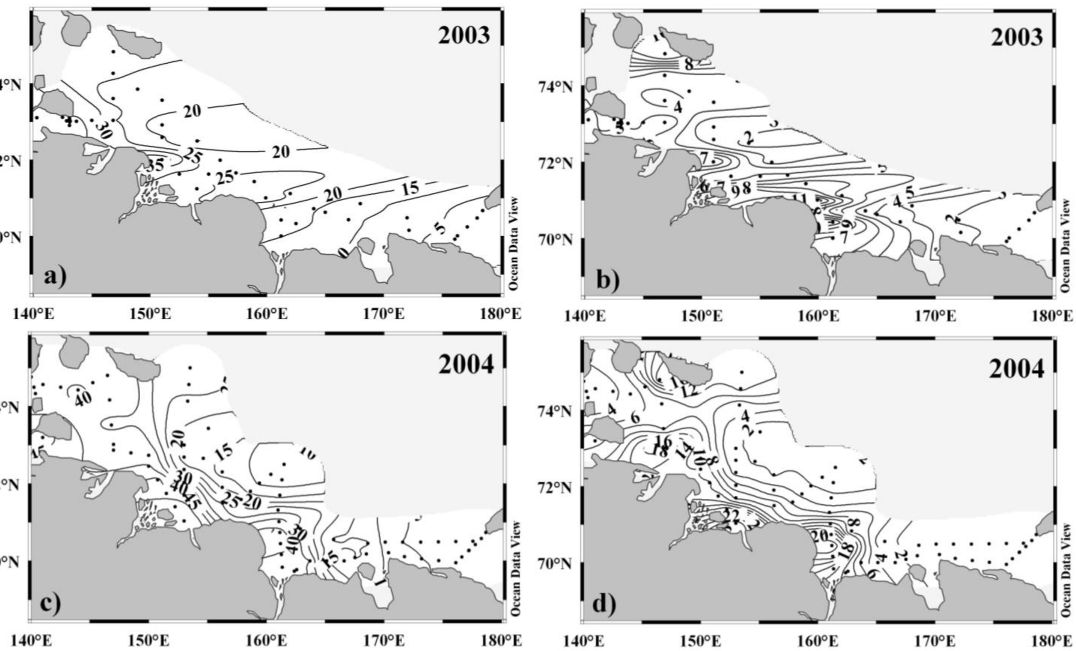

Fig. 11. Spatial distributions of surface water CDOM (µg l^{-1}) **(a, c)** and SPM (mg l^{-1}) **(b, d)** over the ESS shelf during the 2003 and 2004 surveys.

significant role of fluorophores in changing PAR absorption. Thus, in the western part of the ESS a sharp attenuation of PAR was observed within the first several meters of the water column that significantly reduced the depth of the photic layer.

There were some PP measurements done in early September 2000 showing an approximately 7-fold increase from the west to the east: in the west, near the Dm. Laptev Strait, PP was 0.05 g C m^{-2} day^{-1} while in the eastern part of the ESS, near Long Strait, it was 0.30–0.41 g C m^{-2} day^{-1} (unpublished data from I. Umbrumaynts, Institute of Global Climate and Ecology of Roshydromet and RAS). During the summer of 2000 the atmospheric circulation pattern was similar to that in the summer of 2008 (anticyclonic regime) and the eastern ESS was strongly affected by inflow of Pacific-origin water (Savel'eva et al., 2008). Therefore, we can consider these PP values and the spatial distribution in the ESS to be typical of years when high atmospheric pressure dominates over the adjacent Arctic Ocean.

The homogenous density distribution in the western ESS (excluding the near-river-mouth zone) during September 2003 and 2004 (Fig. 6) indicate extensive vertical mixing and was thus an important causal factor for the high pCO_2 values in the surface layer. Note that gas transfer across the thermocline is a major rate-limited process (Matthews, 1999).

As a result of the factors mentioned above, waters in the western region of the ESS were oversaturated in CO_2 compared to atmospheric values and were characterized by net production of inorganic carbon and by CO_2 release to the atmosphere (Fig. 9). Thus, the western part of the ESS represents a river- and thermo-abrasion-dominated heterotrophic area.

The eastern part of the ESS was strongly influenced by waters from the Chukchi Sea, whose biogeochemical conditions were determined by the inflow of transformed waters from the Pacific Ocean (clear, salty, and highly productive, with high nutrient and inorganic carbon content). In the eastern part of the ESS the surface water pCO_2 values were lower than atmospheric pCO_2 values (Fig. 8) as a result of high PP. This is confirmed by high pH and O_2 saturation values (Pipko et al., 2008b; Anderson et al., 2009). The water column exhibited a double-layer structure with a well-defined pycnocline (Fig. 6). Concentrations of all CS parameters differed distinctly between the surface and the bottom layers, as is typical when PP is active in the surface water and decay products from OM mineralization are added to the bottom water. Hence, seawater pCO_2 values in the surface water were low (about 200–270 µatm), while the pCO_2 values in the bottom waters were about 5 times higher, up to 1200 µatm.

Minimum values of about 150–195 µatm were observed in subsurface waters (10–20 m). The O_2 saturation reached a maximum of 138 % at these depths in Long Strait, a region much influenced by high nutrients and clear water from the Pacific Ocean. Such a subsurface maximum of photosynthetic activity is typical for the Chukchi Sea shelf where the upper layer is very clear and light penetrates to the lower layer with sufficient intensity to allow phytoplankton to grow rapidly at depth (Springer and McRoy, 1993). CO_2 fluxes in

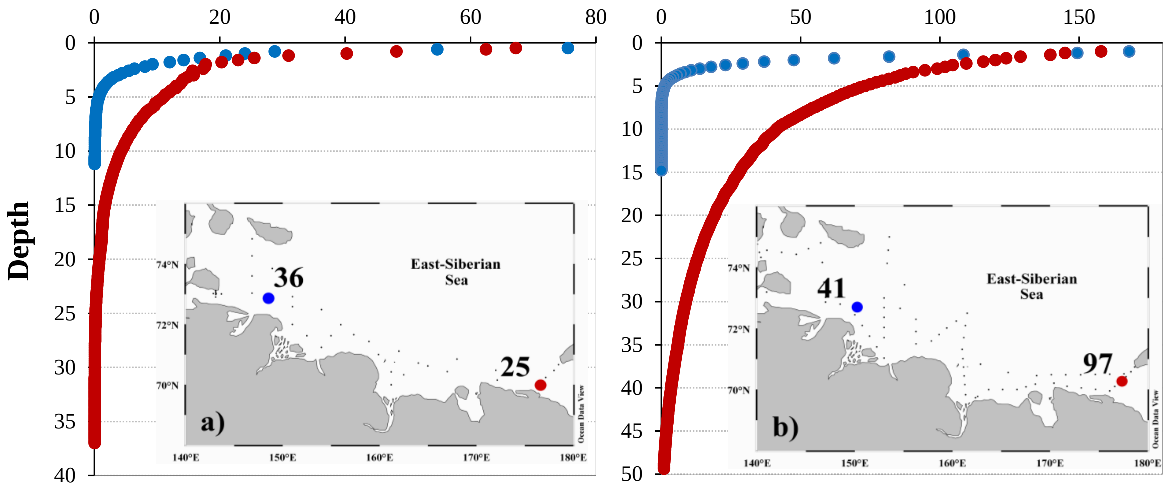

Fig. 12. Profiles of PAR in the ESS in September 2003 **(a)** and September 2004 **(b)**.

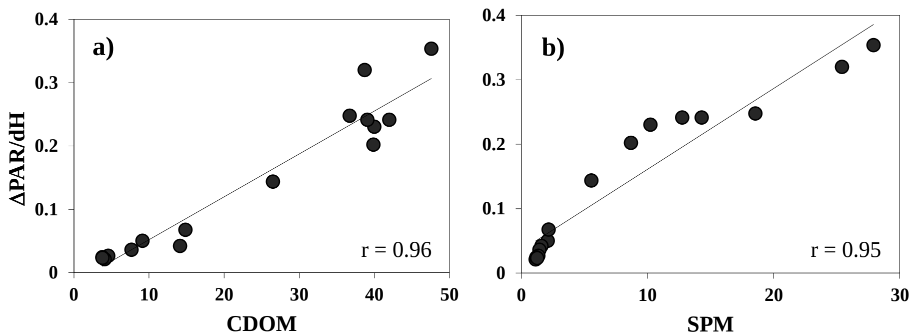

Fig. 13. Correlation of the PAR extinction versus CDOM ($\mu g\,l^{-1}$) **(a)** and SPM ($mg\,l^{-1}$) **(b)** in the H_1 layer.

the eastern part of the ESS were into the sea and ranged from -0.1 to $-5.0\,mmol\,m^{-2}\,day^{-1}$ (Fig. 9). The intensive PP with the resulting absorption of atmospheric CO_2 is evidence of autotrophy in the ESS eastern region.

5.2 Interannual variability

Despite the fact that trends of the spatial pCO$_2$ distribution in the surface water were the same during the summers of 2003, 2004, and 2008 (decrease from west to east), values of pCO$_2$ showed significant interannual variability (Fig. 8). The highest pCO$_2$ values were observed in September 2004 and reached 1033 µatm. The lowest values were obtained in September 2008 in the eastern part of the ESS. The position of the zero CO_2 flux curve also varied substantially between September 2003, 2004, and 2008 (Fig. 9).

The largest year-to-year variability of CS parameters was observed in the central coastal zone of the ESS (Figs. 7, 8, 14). This area is the most dynamic and is distinguished by the interaction of waters with extreme characteristics, from river waters with close-to-zero salinity to typical seawaters (with salinity up to 30 in the surface layer). Strong interannual variability in this area is clearly illustrated in Fig. 14, where profiles of hydrological parameters at the closely-positioned stations are shown. CS characteristics of surface and bottom layers at these stations are presented in Table 3.

The A_T in the river runoff was calculated, using linear regression, as the intercept at zero salinity from the A_T-S relationship obtained using data from the ESS shelf (Fig. 10). The intercept from linear regression estimates the mean A_T for all runoff entering the ESS shelf and the values are very close: 0.50, 0.49, and 0.50 $mmol\,kg^{-1}$ from surveys in 2003, 2004, and 2008, respectively. The major rivers contributing to the ESS are the Lena and Kolyma rivers, and the average annual A_T values in these rivers are about 0.85 and 0.47 $mmol\,kg^{-1}$, respectively (Gordeev et al., 1996). The observed values primarily reflect the influence of late spring/summer riverine waters, taking into account that during this season river waters are characterized by minimal A_T values. Thus, the river end-members are as strongly influenced by the volume of river runoff as they are by the fractions of water from different sources (the Lena or Kolyma rivers).

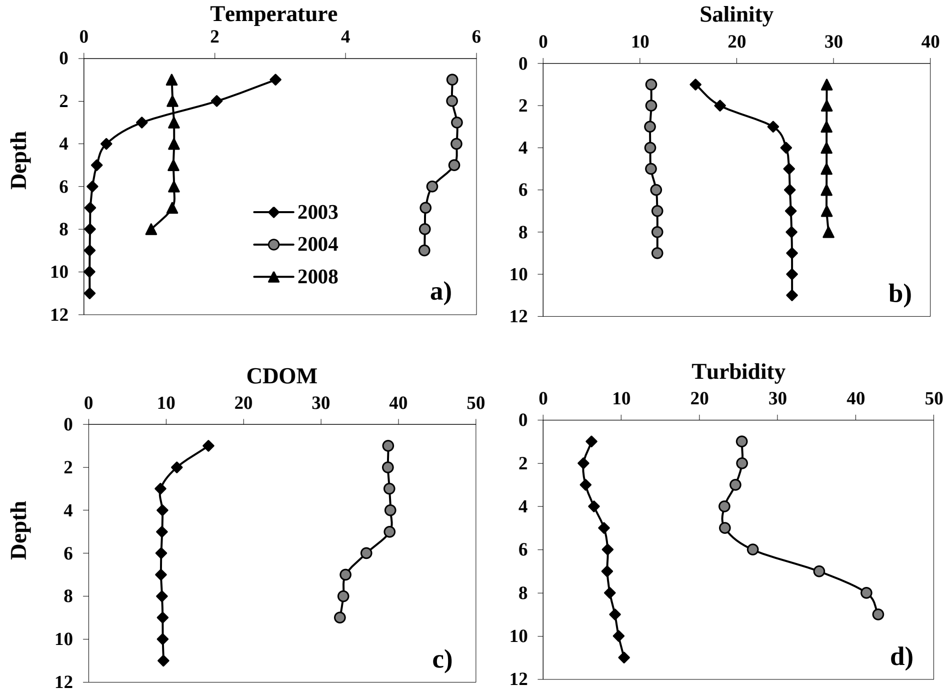

Fig. 14. Profiles of temperature (°C) **(a)**, salinity **(b)**, CDOM ($\mu g\,l^{-1}$) **(c)**, and turbidity (Nephelometric Turbidity Units, NTU) **(d)** at the stations 20, 67 and 33 in September 2003, 2004, and 2008. Coordinates of the stations are pointed in Table 3.

Table 3. Carbon system characteristics of surface/bottom layers at stations 20, 67, and 33.

Year	Station No	Coordinates	A_T, mmol kg^{-1}	$pH_{in\,situ}$, pH units	pCO$_2$, µatm
2003	20	70.001° N, 161.201° E	1.280/1.833	7.766/7.675	521/803
2004	67	70.165° N, 161.270° E	0.975/0.988	7.592/7.593	643/642
2008	33	70.168° N, 161.217° E	2.061/2.064	7.669/7.661	901/919

Table 4. Average river discharge, $m^3\,s^{-1}$, during the summer season (June–September).

Year	Lena River[1]	Kolyma River[2]
2003	38 990	6920
2004	48 564	9535
2008	49 829	7508

[1] Data from http://rims.unh.edu.
[2] Data from the Regional Tiksi Hydrometeorological Service.

The direct river discharge into the ESS, mostly by the Kolyma River, was maximum in the summer of 2004, and minimum in the summer of 2003; the highest discharge of the Lena River was registered in the summer of 2008 and the minimum also occurred in the summer of 2003 (Table 4). At the same time, the river plume in the ESS as traced by the distribution of hydrological parameters, normalized A_T and CDOM, had a maximum easterly extension in 2004 and a minimum in 2008 (Figs. 5, 7, 8, 11). The zone of change in CO_2 flux direction assumed an extreme western position in 2008 and an extreme eastern position in 2004 (Fig. 9). No strong correlation between the volume of river discharge and the interannual dynamics of the CO_2 evasion/invasion areas in the coastal waters of the ESS was observed.

Another factor that determines the interannual dynamics of the CS in the ESS was the dominant atmospheric SLP, which was substantially different in 2003, 2004, and 2008 (Fig. 3). Prevailing along-shore westerly winds over the Laptev Sea and the ESS determined by the dominant field of low atmospheric pressure over the Arctic Ocean in summer 2003 transported the Lena River plume into the ESS and moved the freshened water toward Long Strait. In summer 2004 the strong off-shore winds determined by the interaction of low and high atmospheric pressure centers caused intensive propagation of river waters to the north and east in the ESS and the CO_2 evasion area was at its maximum. In summer 2008 along-shore easterly winds dominated the ESS under the anticyclonic atmospheric regime and resulted in an influx of more saline waters from the Chukchi Sea into the ESS. The Kolyma and Indigirka river runoff plumes were forced to move offshore and westward to the New Siberian Islands and the Laptev Sea. Despite the largest Lena River discharge in September 2008 the low-salinity waters were blocked to the west of the ESS and the CO_2 invasion area was at its maximum (Fig. 9). In spite of considerable annual variability of river discharge, the atmospheric pressure pattern was the major factor that determined the geographic peculiarity of the CS dynamics and CO_2 fluxes of the ESS waters. The atmospheric pressure pattern not only affected the distribution of different source waters, but also the magnitude of coastal erosion. The strongest offshore winds during the three years were in 2004, which along with high riverine discharges, resulted in the highest transport of suspended terrigenous (riverine and erosive) OM into the ESS (Dudarev et al., 2008). The minimum measured SPM concentrations were in 2008 when westward water transport occurred and the input of eroded material to the ESS was the lowest: SPM values were about two times lower in the surface layer (the maximum value were measured in the western part of the sea and reached $6.4\,\mathrm{mg\,kg^{-1}}$) and 4.5 times lower in the bottom layer relative to 2004 (O. V. Dudarev, personal communication, 2010). Note that the organic carbon content in SPM ranges from 6 to 16.3 % (Dudarev et al., 2003, 2006).

The highest absolute CO_2 flux values, calculated using a cubic dependence of gas transport formulation for the daily average wind speed (Wanninkhof and McGillis, 1999), were obtained in September 2004 (Fig. 9, Table 2), the time of maximum wind-speed and the highest difference in $p\mathrm{CO_2}$ in the air and surface water ($\Delta p\mathrm{CO_2}$). The lowest absolute CO_2 flux was found in September 2003 under the cyclonic atmospheric regime when weak winds prevailed over the ESS and the $\Delta p\mathrm{CO_2}$ was the smallest.

The CO_2 evasion values calculated for the ESS shelf in the summer (Table 2) exceed the values obtained both for the continental shelf of high latitudes and, in the majority of cases, for the tropical/subtropical seas (Chen and Borges, 2009). This indicates the significant role of allochtonous eroded carbon in the exchange processes in the Arctic shelves, especially in the predominantly heterotrophic western ESS ecosystem.

Previous estimates of the net CO_2 flux have relied on indirect mass balance considerations (Lyakhin and Rusanov, 1983; Anderson et al., 1998a, b; Fransson et al., 2001). All these annual rates of net CO_2 flux have considerable uncertainty. The data reported here represent the first air-sea CO_2 flux considerations for the ESS shelf based on measured CS characteristics and atmospheric $p\mathrm{CO_2}$ during three repeated oceanographic surveys over the ice-free ESS. However, it should be noted that these calculations have caveats too. First, as pointed out above, there are errors in calculated $p\mathrm{CO_2}$ values ($<10\,\mu\mathrm{atm}$) even if they are small compared to the range of $\Delta p\mathrm{CO_2}$ (Table 2). More significant discrepancies are in the assessment of air-sea flux when using different parameterizations of gas transfer velocity or averaging of wind speed (Wanninkhof and McGillis, 1999; Bates and Merlivat, 2001; Feely et al., 2001). Thus, it is important to use the same methods for CO_2 flux comparison. Additional uncertainties arise when spatial averaging is carried out because of interpolation and extrapolation of hydrocast data. Part of the ESS is covered by ice even during the warm season, also resulting in an uncertainty (of 5 %, www.aari.ru) in evaluating the ice-edge position. Finally an uncertainty is associated with scaling up the data to monthly and yearly fluxes, an uncertainty that both is coupled to the sea ice distribution as well as to the $p\mathrm{CO_2}$ evolution with time in the surface water.

The mean values of air CO_2 fluxes for the ice-free ESS in September 2003 and 2004 and August–September 2008 were $0.9\pm0.8\,\mathrm{mmol\,m^{-2}\,day^{-1}}$, $11.5\pm7.5\,\mathrm{mmol\,m^{-2}\,day^{-1}}$, and $0.8\pm2.9\,\mathrm{mmol\,m^{-2}\,day^{-1}}$, respectively. Based on these values, the ice-edge position, the duration of the ice-free period (50, 35, and 50 days for 2003, 2004, and 2008, www.aari.ru), and the area of the ESS $913\times10^3\,\mathrm{km^2}$, we assessed the emission of CO_2 from the ESS during the warm season to an outgassing of 0.4 to $2.3\times10^{12}\,\mathrm{g\,C}$.

We could speculate that this rate is roughly equivalent to an annual flux (0.1 to $0.4\,\mathrm{mol\,m^{-2}\,yr^{-1}}$), ignoring the CO_2 fluxes across the sea ice and thus suggesting that sea ice provides an effective barrier to gas exchange during the major part of the year (Bates and Mathis, 2009, and references therein). However, recent sea-ice studies demonstrate that sea ice is an active participant in the carbon cycle of polar waters and that CO_2 fluxes obtained over seasonal sea ice are far greater than previously reported (Semiletov et al., 2004, 2007; Nomura et al., 2010; Miller et al., 2011; Papakyriakou and Miller, 2011). A winter-time series of measurements of the inorganic carbon system above, within, and beneath the landfast sea ice of the southern Beaufort Sea identified significant vertical CO_2 fluxes, mostly upward away from the ice but with short periods of downward fluxes as well (Miller et al., 2011). Uptake of CO_2 during spring time was generally associated with warming in the presence of high winds ($>6\,\mathrm{m\,s^{-1}}$), while cooling (ice temperature less than $-6\,^{\circ}\mathrm{C}$) and low winds gave rise to CO_2 effluxes (Papakyriakou and Miller, 2011). The next uncertainty is related to the flaw polynyas as their combined area in the ESS is about 5 % of the ESS total, and their lifetime ranges from 90 to 174 days per year (Popov and Karelin, 2009). It has been reported that polynyas, areas of high biological productivity and active ice formation, are generally sinks of CO_2 where CO_2 is drawn into the water both by coupling with organic carbon export and by high solubility in the cold waters typical of polynyas (Anderson et al., 2004; Miller and DiTullio, 2007). However, for highly river-dominated shelf waters, winter mixing with CO_2-rich subsurface waters is highly likely to create conditions favouring the potential for surface waters to outgas CO_2 during winter through polynyas and leads (Bates and Mathis, 2009) because the polynya-induced vertical mixing may act as a drainage of the underlying layers (Dmitrenko et al., 2010). At the same time, fall-season ice growth and wintertime ice production in polynyas might result in an ice-driven carbon pump (Rysgaard et al., 2007). But is this true for the freshened waters of the shallow shelf, where close interactions between sediments, water column, and atmosphere occur?

In September 2008 when Pacific-origin water was substantial in the ESS the potential CO_2 out-gassing was reported to be $\sim 5.5 \times 10^{12}$ g C (Anderson et al., 2009). This value can significantly change from year to year depending upon the input of eroded carbon, which is determined by river runoff and the meteorological regime. Thus, net CO_2 flux to the atmosphere could be strongly enhanced during fall convection. An additional source of CO_2 into the East Siberian Arctic shelf waters might be oxidation of methane (Shakhova et al., 2010a, b); moreover, it is expected that methane emission will increase dramatically in response to the recent warming which is most pronounced in the Arctic.

6 Summary and conclusions

The shelf of the ESS is among the most dynamic of the arctic seas, with substantial interaction and transformation of waters from different sources. Water dynamics is driven by winds (direction and intensity) which are largely dependent upon the location of the surface atmospheric pressure anomalies (atmospheric active centers). This impact on water-mass mixing and current pattern also influences the dynamics of the air-sea CO_2 exchange. The year-to-year dynamics in surface water CS parameters as well as air-sea flux is highly variable. During the period of observation the highest out-gassing of CO_2 was observed in September 2004, when the atmospheric pressure field determined winds predominantly from the south. Thus the river waters were distributed throughout the ESS, supporting a lateral transfer of organic and inorganic carbon from erosion and river runoff. This caused a combination of high air-sea $p$$CO_2$ gradients and high wind speed, resulting in a large out-gassing of CO_2 to the atmosphere. The high flux was also supported by the fact that in 2004 the largest river discharge into the ESS occurred.

The maximum CO_2 uptake by the coastal waters of the ESS was observed in September 2008 when the wind pattern caused a significant inflow of highly transparent water of Pacific origin into the eastern ESS. The hydrographic conditions supported a marine-dominated ecosystem in the eastern ESS with significant PP, resulting in CO_2 consumption leading to low $p$$CO_2$. However, in 2008 the wind conditions were relatively calm resulting in a modest CO_2 uptake from the atmosphere in the eastern part of the sea; the resulting CO_2 flux was slightly positive. The average CO_2 air-sea flux values were the lowest in 2003 when the low atmospheric pressure field dominated the adjacent Arctic Ocean.

This study of the CS in the ESS, including the air-sea CO_2 fluxes, supports the existence of two biogeochemical domains. Furthermore it shows the dominating heterotrophic character of the coastal zone, except for the time when the wind pattern causes substantial inflow of highly productive waters of Pacific origin. The continental shelf pump, a mechanism that sequesters and transfers atmospheric CO_2 into the open ocean, was identified only in the eastern part of the sea (Anderson et al., 2010) when productive waters of the Chukchi Sea strongly influenced this region. The ESS shallow shelf as a whole is a net source of CO_2 into the atmosphere with the efflux ranging from $\sim$0.4 to 2.3×10^{12} g C. This pattern may be strongly modulated by recent warming in the Arctic given the large stores of carbon in northern high-latitude permafrost and positive feedbacks between temperature rise and terrestrial bio-available OM release onto the Arctic shelf.

Considering the dynamics of the ESS there are many uncertainties in the present CO_2 flux evaluations, especially in the light of the rapid climate change in this part of the Arctic. Except for the need of more comprehensive investigations in this still under-studied region of the Arctic Ocean shelf, there also is a need to expand the seasonal and areal coverage.

Acknowledgements. This work was supported by the Far-Eastern Branch of the Russian Academy of Sciences (RAS), the International Arctic Research Center (IARC) of the University of Alaska Fairbanks, and by the NOAA (NA08OAR4600758, IPS) and the National Science Foundation (Nos. OPP-0327664, OPP-0230455, IPS, and OPP-1023281, IPS), all with the University of Alaska. This research was funded in part by the Russian Foundation for Basic Research (No. 10-05-00996-a (IPS), No. 05-05-64213, 08-05-00184, 11-05-00781 (IIP)). This work was also greatly assisted by logistical support from the Knut and Alice Wallenberg Foundation and from the Swedish Polar Research Secretariat. It was also supported by the Swedish Research Council and the European Union projects CarboOcean (contract no. 511176-2), DAMOCLES (contract 018509-2), and EPOCA (contract 211384). We also thank Anatoly Salyuk for providing meteorological data, Oleg Dudarev for providing SPM data, and Candace O'Connor for English editing.

Edited by: Ö. Gustafsson

References

ACIA (Arctic Climate Impact Assessment): Overview Report, Cambridge Univ. Press, Cambridge, 140 pp., 2004.

Alling, V., Sanchez-Garcia, L., Porcelli, D., Pugach, S., Vonk, J. E., van Dongen, B., Morth, C.-M., Anderson, L. G., Sokolov, A., Andersson, P., Humborg, C., Semiletov, I., and Gustafsson, Ö.: Non-conservative behavior of dissolved organic carbon across the Laptev and East Siberian seas, Global Biogeochem. Cy., 24, GB4033, doi:10.1029/2010GB003834, 2010.

Amon, R. M. W. and Benner, R.: Bacterial utilization of different size classes of dissolved organic matter, Limnol. Oceanogr., 41(1), 41–51, 1996.

Anderson, L. G. and Jones, E. P.: Measurements of total alkalinity, calcium and sulfate in natural sea ice, J. Geophys. Res., 90, 9194–9198, 1985.

Anderson, L. G., Olsson, K., and Chierici, M.: A carbon budget for the Arctic Ocean, Global Biogeochem. Cy., 12, 455–465, 1998a.

Anderson, L. G., Olsson, K., Jones, E. P., Chierici, M., and Fransson, A.: Anthropogenic carbon dioxide in the Arctic Ocean: Inventory and sinks, J. Geophys. Res., 103, 27707–27716, 1998b.

Anderson, L. G., Jutterström, S., Kaltin, S., Jones, E. P., and Björk, G.: Variability in river runoff distribution in the Eurasian Basin of the Arctic Ocean, J. Geophys. Res., 109, C01016, doi:10.1029/2003JC001773, 2004.

Anderson, L. G., Jutterström, S., Hjalmarsson, S., Wahlström, I., and Semiletov, I.: Out-gassing of CO_2 from Siberian Shelf seas by terrestrial organic matter decomposition, Geophys. Res. Lett., 36, L20601, doi:10.1029/2009GL040046, 2009.

Anderson, L. G., Tanhua, T., Björk, G., Hjalmarsson, S., Jones, E. P., Jutterström, S., Rudels, B., Swift, J.H., and Wahlström, I.: Arctic ocean shelf-basin interaction: An active continental shelf CO_2 pump and its impact on the degree of calcium carbonate solubility, Deep-Sea Res. Pt. I, 57, 869–879, 2010.

Anderson, L. G., Björk, G., Jutterström, S., Pipko, I., Shakhova, N., Semiletov, I., and Wåhlström, I.: East Siberian Sea, an Arctic region of very high biogeochemical activity, Biogeosciences, 8, 1745–1754, doi:10.5194/bg-8-1745-2011, 2011.

Antonov, V. S.: Distribution of riverine waters in the Arctic Seas, Trudi AANII, 208(2), 25–52, 1957 (in Russian).

Atlas of the Oceans, edited by: Gorshkov, S. G., The Arctic Ocean, vol. III, Head Department of Navigation and Oceanography, Russia, 184 pp., 1980 (in Russian).

Bates, N. R. and Mathis, J. T.: The Arctic Ocean marine carbon cycle: evaluation of air-sea CO_2 exchanges, ocean acidification impacts and potential feedbacks, Biogeosciences, 6, 2433–2459, doi:10.5194/bg-6-2433-2009, 2009.

Bates, N. R. and Merlivat, L.: The influence of short-term wind variability on air-sea CO_2 exchange, Geophys. Res. Lett., 28(17), 3281–3284, 2001.

Bates, N. R., Mathis, J. T., and Jeffries, M. A.: Air-sea CO_2 fluxes on the Bering Sea shelf, Biogeosciences, 8, 1237–1253, doi:10.5194/bg-8-1237-2011, 2011.

Berger, V. Ya. and Primakov, I. M.: Assessment of primary production in the White Sea, Russ. J. Mar. Biol., 33(1), 49–53, 2007.

Borges, A. V., Schiettecatte, L.-S., Abril, G., Delille, B., and Gazeau, F.: Carbon dioxide in European coastal waters, Estuar. Coast. Shelf S., 70, 375–387, 2006.

Bruevich, S. V.: Instruction for Chemical Investigation of Seawater, Glavsevmorput, Moscow, 83 pp., 1944 (in Russian).

Burenkov, V. I., Vedernikov, V. I., Ershova, S. V., Kopelevich, O. V., and Sheberstov, S. V.: Use of data from satellite ocean color scanner SeaWiFS for assessment of bio-optical characteristics of the Barents Sea, Oceanology, 41(4), 461–468, 2001.

Cai, W.-J., Wang, Zh. A., and Wang, Y.: The role of marsh-dominated heterotrophic continental margins in transport of CO_2 between the atmosphere, the land-sea interface and the ocean, Geophys. Res. Lett., 30, 16, 1849, doi:10.1029/2003GL017633, 2003.

Carmack, E., Barber, D., Christensen, J., Macdonald, R., Rudels, B., and Sakshaug, E.: Climate variability and physical forcing of the food webs and the carbon budget on panarctic shelves, Prog. Oceanogr., 71, 145–181, 2006.

Chen, C. T. A. and Borges, A. V.: Reconciling opposing views on carbon cycling in the coastal ocean: Continental shelves as sinks and near-shore ecosystems as sources of atmospheric CO_2, Deep-Sea Res. Pt. II, 56(8–10), 578–590, 2009.

Cooper, L. W., McClelland, J. W., Holmes, R. M., Raymond, P. A., Gibson, J. J., Guay, C. K., and Peterson, B. J.: Flow-weighted values of runoff tracers (δ^{18}O, DOC, Ba, alkalinity) from the six largest Arctic rivers, J. Geophys. Res., 35, L18606, doi:10.1029/2008GL035007, 2008.

Dickson, A. G. and Millero, F. J.: A comparison of the equilibrium constants for the dissociation of carbonic acid in seawater media, Deep-Sea Res., 34, 1733–1743, 1987.

Dittmar, T. and Kattner, G.: The biogeochemistry of the river and shelf ecosystem of the Arctic Ocean: A review, Mar. Chem., 83, 103–120, 2003.

Dmitrenko, I., Kirillov, S., Eicken, H., and Markova, N.: Wind-driven summer surface hydrology of the eastern Siberian Shelf, Geophys. Res. Lett., 32, L14613, doi:10.1029/2005GL023022, 2005.

Dmitrenko, I. A., Kirillov, S. A., and Tremblay, L. B.: The longterm and interannual variability of summer fresh water storage over the eastern Siberian shelf: Implication for climatic change, J. Geophys. Res., 113, C03007, doi:10.1029/2007JC004304, 2008.

Dmitrenko, I. A., Kirillov, S. A., Tremblay, L. B., Bauch, D., Hölemann, J. A., Krumpen, T., Kassens, H., Wegner, C., Heinemann, G., and Schröder, D.: Impact of the Arctic Ocean Atlantic water layer on Siberian shelf hydrography, J. Geophys. Res., 115, C08010, doi:10.1029/2009JC006020, 2010.

DOE: Handbook of Methods for the Analysis of the Various Parameters of the Carbon Dioxide System in Sea Water, Version 2, edited by: Dickson, A. G. and Goyet, C., 1994.

Dudarev, O. V., Botsul, A. I., Semiletov, I. P., and Charkin, A. N.: Present-day sedimentation in the coastal-shelf cryolithozone of the Dmitry Laptev Strait, the East Siberian Sea, Tikhookean. Geol., 22, 1, 51–60, 2003.

Dudarev, O. V., Semiletov, I. P., Charkin, A. N., and Botsul, A. I.: Deposition settings on the Continental Shelf of the East Siberian Sea, Dokl. Earth Sci., 409A(6), 1000–1005, 2006.

Dudarev, O. V., Charkin, A. N., Semiletov, I. P., Shilo, I. N., Salyuk, A. N., and Spivak, E. A.: The current state of submarine island relicts on the East Siberian shelf, Dokl. Earth Sci., 419(1), 352–358, 2008.

Dudarev, O. V., Charkin, A. N., Semiletov, I. P., and Gustafsson, Ö.: About thin lamination near-bottom suspended flows on the East Siberian Sea shelf, in: Proceedings of an international scientific conference dedicated to 100 years since the birth of D.G. Panov, 8–11 June 2009, Rostov-on-Don, Russia, 106–109, 2009.

Fransson, A., Chierici, M., Anderson, L. C., Bussmann, I., Kattner, G., Jones, E. P., and Swift, J. H.: The importance of shelf processes for the modification of chemical constituents in the waters of the Eurasian Arctic Ocean: Implications for carbon fluxes, Cont. Shelf Res., 21, 225–242, 2001.

Feely, R. A., Sabine, C. L., Takahashi, T., and Wanninkhof, R.:

Uptake and storage of carbon dioxide in the oceans: The global CO_2 survey, Oceanography, 14, 18–32, 2001.

Gavrilov, A. V.: Geocryological typification of Arctic shelves according to the frozen strata formation, Earth's Cryosphere, XII, 3, 69–79, 2008 (in Russian).

Gordeev, V. V., Martin, J. M., Sidorov, I. S., and Sidorova, M. V.: A reassessment of the Eurasian river input of water, sediment, major elements, and nutrients to the Arctic Ocean, Am. J. Sci., 296, 664–691, 1996.

Grigoriev, M. N.: Morphology and dynamics of sub-sea permafrost evolution in the coastal-shelf zone of the Laptev and East Siberian seas, Science and Education, 4, 104–109, 2006 (in Russian).

Grigoriev, M. N. and Rachold, V.: The degradation of coastal permafrost and the organic carbon balance of the Laptev and East Siberian seas, in: Proceedings of the 8th International Conference on Permafrost, 21–25 July 2003, Zurich, Switzerland, 1, 319–324, 2003.

Grigoriev, M. N., Razumov, S. O., Kunitzkiy, V. V., and Spektor, V. B.: Dynamics of the Russian East Arctic Sea coast: Major factors, regularities and tendencies, Earth's Cryosphere, X, 4, 74–94, 2006 (in Russian).

Guo, L., Semiletov, I., Gustafsson, Ö., Ingri, J., Andersson, P., Dudarev, O., and White, D.: Characterization of Siberian Arctic coastal sediments: Implications for terrestrial organic carbon export, Global Biogeochem. Cy., 18, GB1036, doi:10.1029/2003GB002087, 2004.

Gustafsson, Ö., van Dongen, B. E., Vonk, J. E., Dudarev, O. V., and Semiletov, I. P.: Widespread release of old carbon across the Siberian Arctic echoed by its large rivers, Biogeosciences, 8, 1737–1743, doi:10.5194/bg-8-1737-2011, 2011.

Haraldsson, C., Anderson, L. G., Hassellov, M., Hulth, S., and Olsson, K.: Rapid, high-precision potentiometric titration of alkalinity in ocean and sediment pore waters, Deep-Sea Res. Pt. I, 44(12), 2031–2044, 1997.

Johnson, M. A. and Polyakov, I.: The Laptev Sea as a source for recent Arctic Ocean salinity change, Geophys. Res. Lett., 28(10), 2017–2020, 2001.

Jutterström, S. and Anderson, L. G.: Uptake of CO_2 by the Arctic Ocean in a changing climate, Mar. Chem., 122, 96–104, 2010.

Kulakov, M., Stanovoy, V., and Kirillov S.: Oceanography of the East-Siberian Sea, Proc. of the ESSS Workshop 2003, Malaga, Spain, 11–18 October 2003.

Lewis, E. and Wallace, D. W. R.: Program developed for CO_2 system calculations, ORNL/CDIAC-105, Carbon Dioxide Information Analysis Center, Oak Ridge National Laboratory, U.S. Department of Energy, Oak Ridge, Tennessee, 1998.

Lyakhin, Yu. I. and Rusanov, V. P.: Exchange of oxygen and carbon dioxide between Arctic Ocean and atmosphere, Dokl. Earth Sci., 271(1), 198–201, 1983 (in Russian).

Macdonald, R. W., Anderson, L. G., Christensen, J. P., Miller, L. A., Semiletov, I. P., and Stein, R.: The Arctic Ocean: Budgets and fluxes, in: Carbon and Nutrient Fluxes in Continental Margins: A Global Synthesis, edited by: Liu, K.-K., Atkinson, L., Quinones, R., and Talaue-McManus, L., Springer, Heidelberg, Germany, 291–303, 2010.

Matthews, B. J. H.: The Rate of Air-Sea CO_2 Exchange: Chemical Enhancement and Catalysis by Marine Microalgae, Ph.D. thesis, School of Environmental Sciences, University of East Anglia, Norwich, 1999.

McGuire, A. D., Anderson, L. G., Christensen, T. R., Dallimore, S., Guo, L., Hayes, D. J., Heimann, M., Lorenson, T. D., Macdonald, R. W., and Roulet, N.: Sensitivity of the carbon cycle in the Arctic to climate change, Ecol. Monogr., 79, 523–555, 2009.

Mehrbach, C., Culberson, C. H., Hawley, J. E., and Pytkowicz, R. M.: Measurement of the apparent dissociation constants of carbonic acid in seawater at atmospheric pressure, Limnol. Oceanogr., 18, 897–907, 1973.

Miller, L. A. and DiTullio, G. R.: Gas Fluxes and Dynamics in Polynyas, in: Polynyas: Windows to the World, edited by: Smith Jr., W. O. and Barber, D. G., Elsevier Oceanography Series, Elsevier, Amsterdam, 74, 163–91, 2007.

Miller, L. A., Papakyriakou, T. N., Collins, R. E., Deming, J. W., Ehn, J., Macdonald, R. W., Mucci, A., Owens, O., Raudsepp, M., and Sutherland, N.: Carbon dynamics in sea ice: A winter flux time series, J. Geophys. Res., 116, C02028, doi:0.1029/2009JC006058, 2011.

Nedashkovsky, A. P., Khvedynich, S. V., and Petrovsky, T. V.: Alkalinity of sea ice in the high-latitudinal arctic according to the surveys performed at North Pole drifting station 34 and characterization of the role of the arctic ice in the CO_2 exchange, Oceanology, 49(1), 55–63, 2009.

Nikiforov, Ye. G. and Shpaikher, A. O.: Features of the Formation of Hydrological Regime Large Scale Variations in the Arctic Ocean, Hydrometeoizdat, Leningrad, 269 pp., 1980 (in Russian).

Nomura, D., Eicken, H., Gradinger, R., and Shirasawa, K.: Rapid physically driven inversion of the air–sea ice CO_2 flux in the seasonal land fast ice off Barrow, Alaska after onset of surface melt, Cont. Shelf Res., 30(19), 1998–2004, 2010.

Olsson, K. and Anderson, L.: Input and biogeochemical transformation of dissolved carbon in the Siberian Shelf seas, Cont. Shelf Res., 17(7), 819–833, 1997.

Papakyriakou, T. and Miller, L.: Springtime CO_2 exchange over seasonal sea ice in the Canadian Arctic Archipelago, Ann. Glaciol., 52(57), 215–224, 2011.

Pavlova, G. Yu., Tishchenko, P. Ya., Volkova, T. I., Dickson, A., and Wallmann, K.: Intercalibration of Bruevich's method to determine the total alkalinity in seawater, Oceanology, 48(3), 460–465, 2008.

Pipko, I. I., Semiletov, I. P., and Pugach, S. P.: The carbonate system of the East Siberian Sea waters, Dokl. Earth Sci., 402(4), 624–627, 2005.

Pipko, I. I., Repina, I. A., Salyuk, A. N., Semiletov, I. P., and Pugach, S. P.: Comparison of calculated and measured CO_2 fluxes between the ocean and atmosphere in the southwestern part of the East Siberian Sea, Dokl. Earth Sci., 422(7), 1105–1108, 2008a.

Pipko, I., Semiletov, I. P., Tishchenko, P. Ya., Pugach, S. P., and Savel'eva, N. I.: Variability of the carbonate system parameters in the coast-shelf zone of the East Siberian Sea during the autumn season, Oceanology, 48(1), 54–67, 2008b.

Pipko, I. I., Pugach, S. P., and Semiletov, I. P.: The autumn distribution of the CO_2 partial pressure in bottom waters of the East Siberian Sea, Dokl. Earth Sci., 425(2), 345–349, 2009.

Popov, A. V. and Karelin, I. D.: Role of the Arctic flaw polynyas in genesis of new ice in the seas of the Siberian shelf and freshening of the surface waters of the Arctic Ocean, Problems of Arctic and Antarctic, 3(83), 74–87, 2009.

Proshutinsky, A. Y. and Johnson, M. A.: Two circulation regimes of the wind-driven Arctic Ocean, J. Geophys. Res., 102(C6), 12493–12514, 1997.

Pugach, S. P., Pipko, I. I., and Semiletov, I. P.: Distribution of CDOM in the East-Siberian Sea, in: Proceedings of the 24th International Symposium on the Okhotsk Sea and Sea Ice, Mombetsu, Japan, 15–20 February 2009, 194–197, 2009.

Pugach, S. P., Semiletov, I. P., and Pipko, I. I.: Tracing river runoff and DOC over the East-Siberian Shelf using in situ CDOM measurements, Geophys. Res. Abstr., 12, EGU2010-3793, EGU General Assembly, 2010.

Rachold, V.: The Role of Coastal Processes in the Arctic System, ARCUS 16th Annual Meeting and Arctic Forum, Washington DC (USA), 13–14 May 2004, 2004.

Rachold, V., Bolshiyanov, D. Y., Grigoriev, M. N., Hubberten, H.-W., Junker, R., Kunitsky, V. V., Merker, F., Overduin, P., and Schneider, W.: Nearshore Arctic subsea permafrost in transition, Eos Trans. AGU, 88, 149–156, doi:10.1029/2007EO130001, 2007.

Razumov, S. O.: Permafrost as a factor of coastal zone dynamics in the East Arctic seas of Russia, Oceanology, 50(2), 285–291, 2010 (in Russian).

Romankevich, E. A., Korneeva, G. A., Shevchenko, V. P., Gordeev, V. Yu., and Belyaev, N. A.: Particulate organic matter in the Barents Sea, Oceanology, 40(2), 208–216, 2000 (in Russian).

Romanovskii, N. N., Hubberten, H.-W., Gavrilov, A. V., Eliseeva, A. A., and Tipenko, G. S.: Offshore permafrost and gas hydrate stability zone on the shelf of East Siberian Seas, Geo.-Mar. Lett., 25, 167–182, 2005.

Rysgaard, S., Glud, R. N., Sejr, M. K., Bendtsen, J., and Christensen, P. B.: Inorganic carbon transport during sea ice growth and decay: A carbon pump in polar seas, J. Geophys. Res., 112, C03016, doi:10.1029/2006jc003572, 2007.

Sakshaug, E.: Primary and secondary production in the Arctic seas, in: The Organic Carbon Cycle in the Arctic Ocean, edited by: Stein, R. and Macdonald, R. W., Springer, New York, 57–81, 2004.

Sanchez-Garcia, L., Alling, V., Pugach, S., Vonk, J., van Dongen, B., Humborg, C., Dudarev, O., Semiletov, I., and Gustafsson, Ö.: Inventories and behavior of particulate organic carbon in the Laptev and East Siberian seas, Global Biogeochem. Cy., 25, GB2007, doi:10.1029/2010GB003862, 2011.

Savel'eva, N. I., Semiletov, I. P., and Pipko, I. I.: Impact of synoptic processes and river discharge on the thermohaline structure in the East Siberian Sea shelf, Russ. Meteorol. Hydrol., 33(4), 240–246, 2008.

Semiletov, I. P.: Destruction of the coastal permafrost as an important factor in biogeochemistry of the Arctic shelf waters, Dokl. Earth Sci., 368, 679–682, 1999a.

Semiletov, I. P.: Aquatic sources and sinks of CO_2 and CH_4 in the Polar Regions, J. Atmos. Sci., 56, 286–306, 1999b.

Semiletov, I. P. and Pipko, I. I.: Sinks and sources of carbon dioxide in the Arctic Ocean: Results of direct instrumental measurements, Dokl. Earth Sci., 414(3), 642–645, 2007.

Semiletov, I. P., Makshtas, A., Akasofu, S.-I., and Andreas, E.: Atmospheric CO_2 balance: The role of Arctic sea ice, Geophys. Res. Lett., 31, L05121, doi:10.1029/2003GL017996, 2004.

Semiletov, I., Dudarev, O., Luchin, V., Charkin, A., Shin, K., and Tanaka, N.: The East-Siberian Sea as a transition zone between the Pacific origin water and local shelf water, Geophys. Res. Lett., 32, L10614, doi:10.1029/2005GL022490, 2005.

Semiletov, I. P., Pipko, I. I., Repina, I., and Shakhova, N. E.: Carbonate chemistry dynamics and carbon dioxide fluxes across the atmosphere-ice-water interfaces in the Arctic Ocean: Pacific sector of the Arctic, J. Marine Syst., 66, 204–206, doi:10.1016/j.jmarsys.2006.05.012, 2007.

Serreze, M. C., Walsh, J. E., Chapin III, F. S., Osterkamp, T., Dyurgerov, M., Romanovsky, V., Oechel, W. C., Morison, J., Zhang, T., and Barry, R. G.: Observational evidence of recent change in the northern high-latitude environment, Climatic Change, 46, 159–209, 2000.

Shakhova, N. E. and Semiletov, I. P.: Characteristic features of carbon cycle in the shallow shelf of the eastern sector of Russian Arctic, in: Environmental and Climate Changes and Catastrophes, Vol. 4, edited by: Laverov, N. P., Institute of Physicochemical and Biological Problems of Soil Science Russian Academy of Sciences, Moscow, 167–181, 2008.

Shakhova, N., Semiletov, I., Salyuk, A., Yusupov, V., Kosmach, D., and Gustafsson, Ö.: Extensive methane venting to the atmosphere from sediments of the East Siberian Arctic Shelf, Science, 327, 1246–1250, 2010a.

Shakhova, N., Semiletov, I., Leifer, I., Rekant, P., Salyuk, A., and Kosmach, D.: Geochemical and geophysical evidence of methane release from the inner East Siberian Shelf, J. Geophys. Res., 115, C08007, doi:10.1029/2009JC005602, 2010b.

Sorokin, Yu. A. and Sorokin, P. Yu.: Plankton and primary production in the Lena River estuary and in the South-eastern Laptev Sea, Estuar. Coast. Shelf S., 43, 399–418, 1996.

Springer, A. M. and McRoy, C. P.: The paradox of pelagic food webs in the northern Bering Sea – III. Patterns of primary production, Cont. Shelf Res., 13, 575–599, 1993.

Stein, R. and Macdonald, R. W. (Eds.): The organic carbon cycle in the Arctic Ocean, Springer-Verlag, Berlin, Germany, 363 pp., 2004.

Thomas, H., Schiettecatte, L.-S., Suykens, K., Koné, Y. J. M., Shadwick, E. H., Prowe, A. E. F., Bozec, Y., de Baar, H. J. W., and Borges, A. V.: Enhanced ocean carbon storage from anaerobic alkalinity generation in coastal sediments, Biogeosciences, 6, 267–274, doi:10.5194/bg-6-267-2009, 2009.

van Dongen, B. E., Semiletov, I., Weijers, J. W. H., and Gustafsson, Ö.: Contrasting lipid biomarker composition of terrestrial organic matter exported from across the Eurasian Arctic by the five Great Russian Arctic Rivers, Global Biogeochem. Cy., 22, GB1011, doi:10.1029/2007GB002974, 2008.

Verspecht, F. and Pattiaratchi, C.: On the significance of wind event frequency for particulate resuspension and light attenuation in coastal water, Cont. Shelf Res., 30, 1971–1982, 2010.

Vetrov, A. A. and Romankevich, E. A.: Carbon cycle in the Russian Arctic seas, Springer Verlag, Berlin, 331 pp., 2004.

Vinogradov, M. E., Vedernikov, V. I., Romankevich, E. A., and Vetrov, A. A.: Some components of carbon cycle in the Russian Arctic seas, Oceanology, 40(2), 221–233, 2000.

Vonk, J. E., Sánchez-García, L., Semiletov, I., Dudarev, O., Eglinton, T., Andersson, A., and Gustafsson, Ö.: Molecular and radiocarbon constraints on sources and degradation of terrestrial organic carbon along the Kolyma paleoriver transect, East Siberian Sea, Biogeosciences, 7, 3153–3166, doi:10.5194/bg-7-3153-2010, 2010.

Wanninkhof, R.: Relationship between wind speed and gas

exchange over the ocean, J. Geophys. Res., 97, 7373–7382, 1992.
Wanninkhof, R. and McGillis, W. R.: A cubic relationship between air-sea CO_2 exchange and wind speed, Geophys. Res. Lett., 26, 1889–1892, 1999.
Weingartner, T. J., Danielson, S., Sasaki, Y., Pavlov, V., and Kulakov, M.: The Siberian Coastal Current: A wind- and buoyancy-forced Arctic coastal current, J. Geophys. Res., 104, 29697–29713, 1999.
Weiss, R.: The solubility of nitrogen, oxygen, and argon in water and seawater, Deep-Sea Res., 17, 721–735, 1970.
Wollast, R.: Evaluation and comparison of the global carbon cycle in the coastal zone and in the open ocean, in: The Sea, edited by: Brink, K. H. and Robinson, A. R., John Wiley & Sons, New York, 10, 213–252, 1998.